**Supporting information:**

# Fluorination-Driven Optimization of Non-Fused Small Molecular Acceptors for High-Efficiency Organic Solar Cells

Shuai Liu,[a] Tongzi Li,[a] Wenzhao Xiong,[a] Jiang Zhou,[a] Xuelong Dai,[a] Yang Yi,[a] Huawei Hu,[*a,b] Yiwang Chen[*a,b]

[a] State Key Laboratory for Modification of Chemical Fibers and Polymer Materials, College of Materials Science and Engineering, Donghua University, Shanghai 201620, China.

E-mail: huaweihu@dhu.edu.cn, ywchen@ncu.edu.cn

Prof. Y. Chen, Prof. H. Hu

[b] Key Lab of Fluorine and Silicon for Energy Materials and Chemistry of Ministry of Education/National Engineering Research Center for Carbohydrate Synthesis, Jiangxi Normal University, 99 Ziyang Avenue, Nanchang 330022, China.

## Molecular properties characterization (UV-vis spectra, TGA, and CV):

The UV-Vis absorption spectra of the solution and film were acquired on a Shimadzu UV-1200 Spectrophotometer. Film samples were spin-cast on ITO substrates. Thermogravimetric analysis (TGA) was carried out on a WCT-2 thermal balance under nitrogen protection at a heating rate of 10 ºC/min. UV-Vis absorption spectra were collected from the solution of the two polymers with a concentration of 0.02 mg/mL in chloroform at different temperatures. Cyclic voltammetry was carried out on a Interface1000E electrochemical workstation with three electrodes configuration, using Ag/AgCl as the reference electrode, a Pt plate as the counter electrode, and a glassy carbon as the working electrode, in a 0.1 mol/L tetrabutylammonium hexafluorophosphate acetonitrile solution. Potentials were referenced to the ferrocenium/ferrocene couple by using ferrocene as external standards in acetonitrile solutions. The HOMO energy levels were determined by $E_{HOMO} = -[q\,(E_{re} - E_{ferrocene}) + 4.8\ eV]$, while the LUMO energy levels were determined by $E_{LUMO} = -[q\,(E_{ox} - E_{ferrocene}) + 4.8\ eV]$.

**Surface Energy:** Contact angle measurements were carried out by an Attension Theta Flex meter, using water and ethylene glycol by sessile drop analysis. The surface tension values of films are calculated according to the previous report[1], in which:

$$\gamma_{Water}(\cos\theta_{Water} + 1) = \frac{4\gamma^{p}_{water}\times\gamma^{p}}{\gamma^{p}_{water}+\gamma^{p}} + \frac{4\gamma^{d}_{water}\times\gamma^{d}}{\gamma^{d}_{water}+\gamma^{d}}$$

$$\gamma_{EG}(\cos\theta_{EG} + 1) = \frac{4\gamma^{p}_{EG}\times\gamma^{p}}{\gamma^{p}_{EG}+\gamma^{p}} + \frac{4\gamma^{d}_{EG}\times\gamma^{d}}{\gamma^{d}_{EG}+\gamma^{d}}$$

$$\gamma = \gamma^{d} + \gamma^{p}$$

where θ is the contact angle of each thin film, and γ is the surface tension of samples, which is equal to the sum of the dispersion ($\gamma^{d}$) and polarity ($\gamma^{p}$) components; $\gamma_{water}$ and $\gamma_{EG}$ are the surface tensions of the water and ethylene glycol; and $\gamma^{d}_{water}$, $\gamma^{p}_{water}$, $\gamma^{d}_{EG}$ and $\gamma^{p}_{EG}$ are the dispersion and polarity components of $\gamma_{Water}$ and $\gamma_{EG}$.

**Fabrication and testing of Polymer:non-fused SMA devices**: The best performance for the polymer:SMA devices was achieved after extensive optimization with an inverted structure of ITO/PEDOT:PSS/polymer:non-fused SMA/PNDIT-$F_3$N/Ag and the details are as follows. Pre-patterned ITO-coated glass with a sheet resistance of ~15 Ω per square was used as the substrate. It was cleaned by sequential sonication in soap DI water, DI water, acetone and isopropanol for 15 min at each step. After ultraviolet/ozone treatment for 60 min, a PEDOT:PSS hole transport layer was prepared by spin coating at 4000 r.p.m. Active layers were spin coated from the polymer:SMAs solution to obtain thicknesses of ~100 nm. Polymer: NFAs active layers were cast from chloroform solution with 7 mg/mL polymer concentration and 1:1.2 D/A ratio. The thermally annealed polymer: NFAs films were then annealed at 100 ºC for 10 min followed by spin coating of a thin layer of PNDIT-$F_3$N. Then the substrates are transferred to the vacuum chamber of a thermal evaporator inside the glove box and 100 nm of Ag was deposited as the top electrode. All cells were measured inside the glove box. For device characterizations, *J-V* characteristics were measured under AM1.5G light (100 mWcm$^{-2}$) using a Class AAA Newport solar simulator. The light intensity was calibrated using a standard Si diode (with KG5 filter, purchased from PV

Measurement) to bring spectral mismatch to unity. *J-V* characteristics were recorded using a Keithley 236 source meter unit. The cell area is defined by a metal mask with an aperture area of 4 $mm^2$ to ensure the accuracy of the current density obtained from the *J–V* measurements.

**Electron and hole mobility measurements**. The electron mobilities were measured using the SCLC method, employing a device architecture of ITO/ZnO/active layer /PNDIT-F3N/Ag The hole-mobilities were measured using a device architecture of ITO/PEDOT:PSS/active layer/$MoO_3$/Ag. The mobilities were obtained by taking current-voltage curves and fitting the results to a space charge limited form, where the SCLC is described by:

$$J = \frac{9\varepsilon_0\varepsilon_r\mu(V_{appl} - V_{bi} - V_s)^2}{8L^3}$$

Where $\varepsilon_0$ is the permittivity of free space, $\varepsilon_r$ is the relative permittivity of the material (assumed to be 3), $\mu$ is the hole mobility and $L$ is the thickness of the film. From the plots of $J^{1/2}$ vs $V_{appl} - V_{bi} - V_s$, electron mobilities can be deduced.

**GIWAXS characterization:** GIWAXS measurements were performed at beamline BL16B1 at the Shanghai Synchrotron Radiation Facility. Samples were prepared on Si substrates using identical blend solutions as those used in devices. The 10 KeV X-ray beam was incident at a grazing angle of 0.13°, which maximized the scattering intensity from the samples. The scattered X-rays were detected using a Dectris Pilatus 1-M photon counting detector. Samples were prepared on Si substrates. In-plane and out-of-plane sector averages were calculated using the Nika software package. The uncertainty for the peak fitting of the GIWAXS data is 0.3 Å. The coherence length was calculated using the Scherrer equation: $CL=2\pi K/\Delta q$, where Δq is the full-width at half-maximum of the peak and K is a shape factor (0.9 was used here).[2]

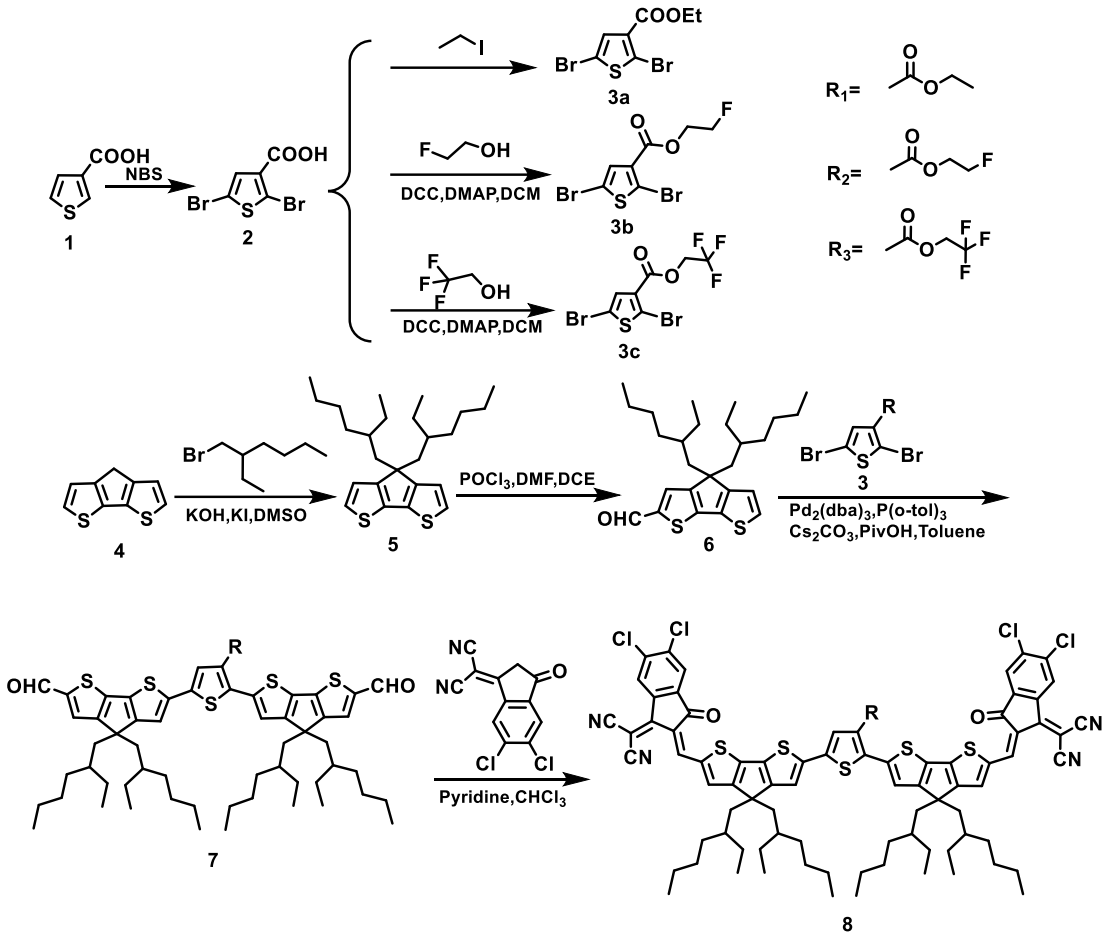


**Scheme S1.** Synthetic routes for ETC-0F, ETC-1F, and ETC-3F.

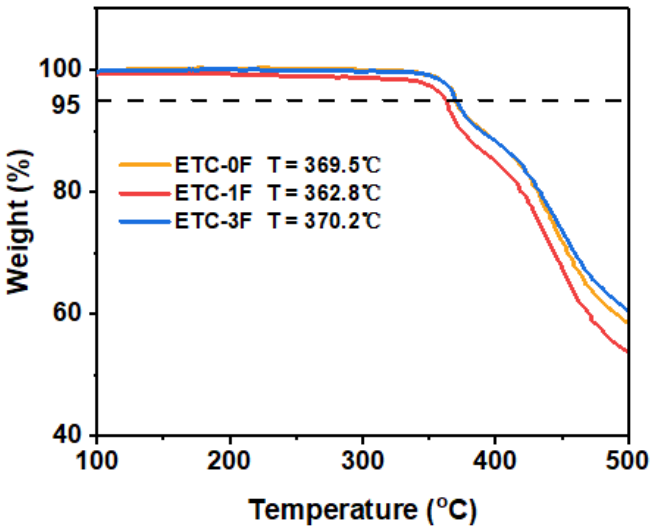


**Figure S1.** Thermogravimetric analysis curve of ETC-0F, ETC-1F, and ETC-3F.

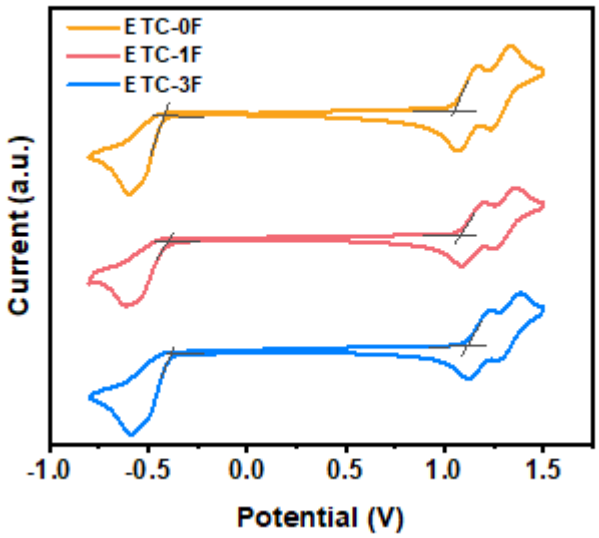


**Figure S2**. The CV plots of ETC-0F, ETC-1F, and ETC-3F.

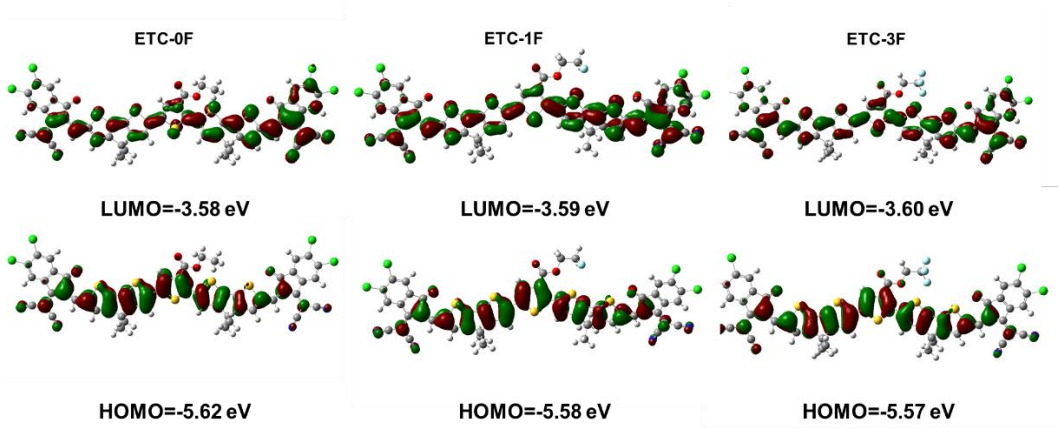


**Figure S3.** The DFT calculated HOMO and LUMO energy levels of ETC-0F, ETC-1F, and ETC-3F.

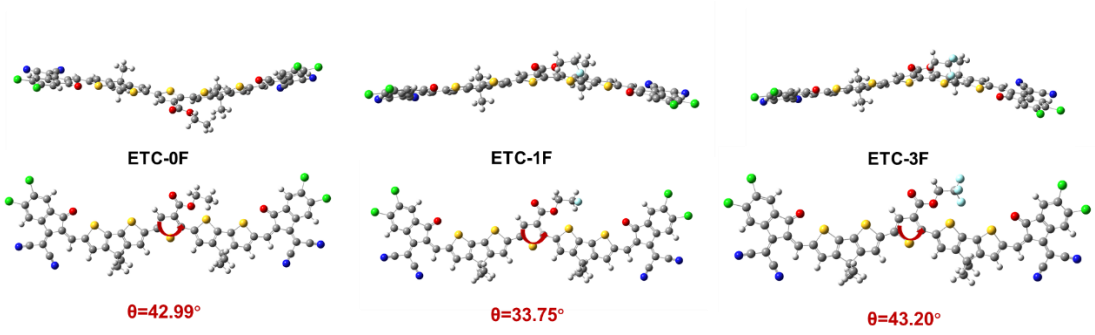


**Figure S4**. Optimized molecular geometries by DFT calculations at B3LYP/6-31G(d) level.

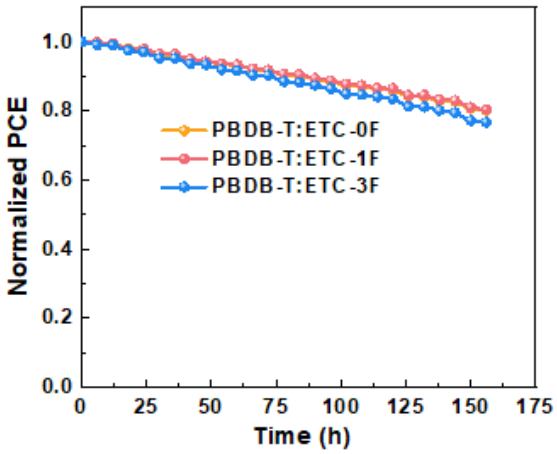


**Figure S5**. Photostability of the encapsulated devices under 1-sun illumination.

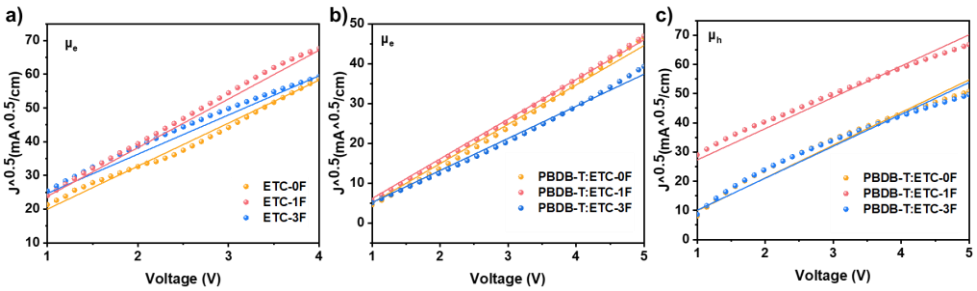


**Figure S6**. (a-b) Electron and (c) Hole current densities with applied voltage in selective carrier injected diodes.

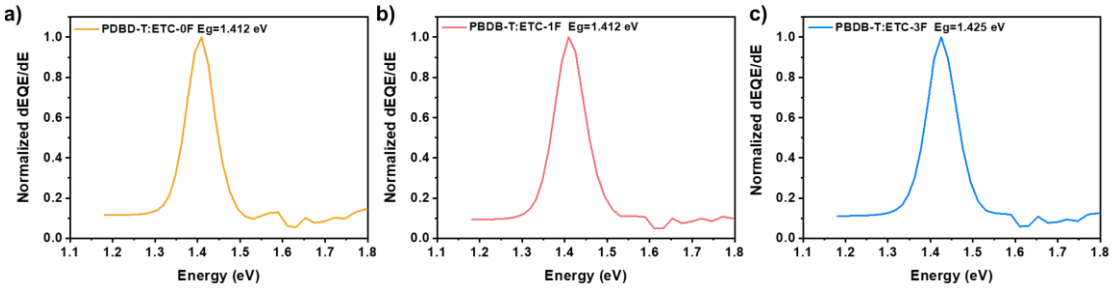


**Figure S7.** Details of optical *E*g determination.

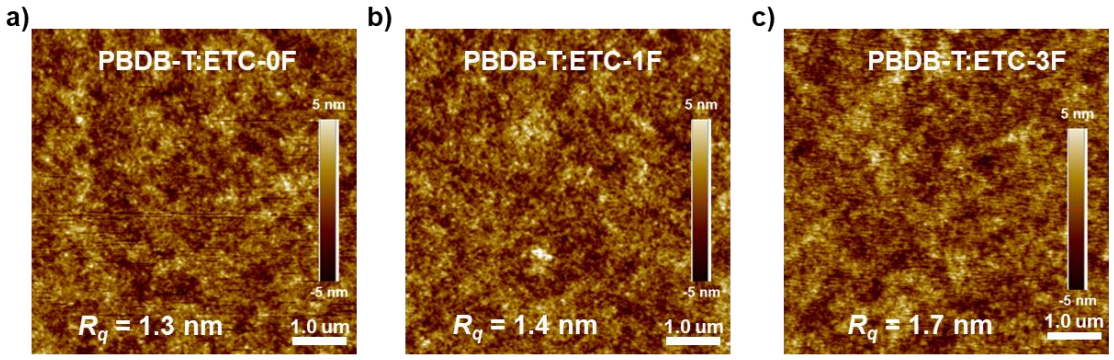


**Figure S8.** AFM images of (a) PBDB-T:ETC-0F, (b) PBDB-T:ETC-1F, and (c) PBDB-T:ETC-3F-based blend films.

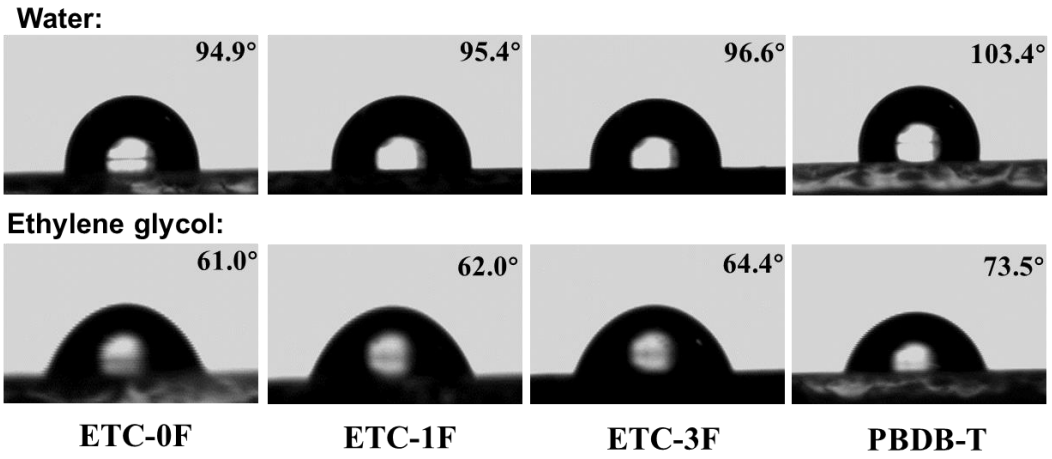


**Figure S9.** Photographs of water and ethylene glycol droplets on the top surface of corresponding films.

**Table S1.** Basic parameters forETC-0F, ETC-1F, and ETC-3F.

| Materials | $\lambda_{max}$ a) [nm] | $\lambda_{max}$ b) [nm] | $\lambda_{onset}$ b) [nm] | $E_g^{opt}$ c) [eV] | LUMO/HOMO d) [eV] | $T_d$ [°C] |
|---|---|---|---|---|---|---|
| ETC-0F | 703 | 717 | 861 | 1.44 | −4.01/−5.48 | 369.5 |
| ETC-1F | 702 | 716 | 860 | 1.44 | −4.03/−5.51 | 362.8 |
| ETC-3F | 690 | 712 | 852 | 1.46 | −4.05/−5.54 | 370.2 |

a) In solution state (Chloroform). b) In pure films. c) Obtained with $E_g^{opt} = 1240/\lambda_{onset}$ b).

d) Measured by cyclic voltammetry (CV) method.

**Table S2.** Device Performance based on PBDB-T:ETC-0F with different D/A ratios.

| D/A ratio (wt/wt) | $V_{OC}$ (V) | $J_{SC}$ (mA cm$^{-2}$) | FF (%) | PCE (%) |
|---|---|---|---|---|
| 1.0:1.0 | 0.77 | 23.20 | 62.45 | 11.16 |
| 1.0:1.2 | 0.77 | 23.81 | 63.80 | 11.70 |
| 1.0:1.5 | 0.77 | 23.74 | 62.69 | 11.46 |

**Table S3.** Device Performance based on PBDB-T:ETC-0F with different amount of DIO additive.

| CN (vol%) | $V_{OC}$ (V) | $J_{SC}$ (mA cm$^{-2}$) | FF (%) | PCE (%) |
|---|---|---|---|---|
| 0 | 0.78 | 22.05 | 54.91 | 9.44 |
| 0.25 | 0.78 | 23.24 | 60.92 | 11.04 |
| 0.50 | 0.77 | 23.81 | 63.80 | 11.70 |
| 0.75 | 0.77 | 23.77 | 63.25 | 11.58 |
| 1.00 | 0.76 | 23.56 | 62.51 | 11.19 |

**Table S4.** Device Performance based on PM6:non-fused SMA-based OSCs.

| Materials | $V_{OC}$ (V) | $J_{SC}$ (mA cm$^{-2}$) | FF (%) | PCE (%) |
|---|---|---|---|---|
| PM6:ETC-0F | 0.87 | 18.76 | 52.25 | 8.57 |
| PM6:ETC-1F | 0.85 | 19.08 | 64.59 | 10.43 |
| PM6:ETC-3F | 0.87 | 16.59 | 43.38 | 6.23 |

**Table S5**. The charge mobility of hole or electron-only devices for corresponding blend films.

| Active layer | $\mu_e$ [$10^{-4}$cm$^2$V$^{-1}$s$^{-1}$] | $\mu_h$ [$10^{-4}$cm$^2$V$^{-1}$s$^{-1}$] | $\mu_h/\mu_e$ |
|---|---|---|---|
| ETC-0F | 4.35 | —— | —— |
| ETC-1F | 5.56 | —— | —— |
| ETC-3F | 3.60 | —— | —— |
| PBDB-T:ETC-0F | 2.59 | 3.65 | 1.41 |
| PBDB-T: ETC-1F | 2.70 | 3.74 | 1.38 |
| PBDB-T: ETC-3F | 1.72 | 3.51 | 2.04 |

**Table S6.** Detailed energy loss analysis of OSCs devices.

| Active layer | $E_g$ (eV) | $V_{OC}$ | $\Delta E_1$ (eV) | $\Delta E_2$ (eV) | $\Delta E_3$ (eV) | $E_{loss}$ (eV) | $EQE_{EL}$ (%) |
|---|---|---|---|---|---|---|---|
| PBDB-T: ETC-0F | 1.412 | 0.77 | 0.262 | 0.050 | 0.330 | 0.642 | $2.92\times10^{-3}$ |
| PBDB-T: ETC-1F | 1.412 | 0.76 | 0.262 | 0.064 | 0.326 | 0.652 | $3.39\times10^{-3}$ |
| PBDB-T: ETC-3F | 1.425 | 0.75 | 0.263 | 0.063 | 0.349 | 0.675 | $1.42\times10^{-3}$ |

**Table S7.** Parameters of out-of-plane and in-plane π-π stacking for donor and acceptor in the corresponding films.

| | Direction | $q$ (Å$^{-1}$) | d (Å) | CCL(Å) |
|---|---|---|---|---|
| ETC-0F | OOP | 1.75 | 3.59 | 23.76 |
| | IP | 0.42 | 14.95 | 29.74 |
| ETC-1F | OOP | 1.76 | 3.57 | 24.72 |
| | IP | 0.43 | 14.60 | 30.54 |
| ETC-3F | OOP | 1.74 | 3.61 | 22.86 |
| | IP | 0.42 | 14.95 | 28.28 |
| PBDB-T:ETC-0F | OOP | 1.75 | 3.59 | 33.68 |
| | IP | 0.32 | 19.63 | 104.04 |
| PBDB-T:ETC-1F | OOP | 1.75 | 3.59 | 34.48 |
| | IP | 0.32 | 19.63 | 1.5.21(修改) |
| PBDB-T:ETC-3F | OOP | 1.74 | 3.61 | 26.50 |
| | IP | 0.32 | 19.63 | 93.36 |

**Table S8.** Surface energy for pure and blend films calculated from water and ethylene glycol contact angle.

| Films | Contact angle(deg) | | surface free energy $\gamma$(mJ $m^{-2}$) | $\chi$donor-acceptor (K) |
|---|---|---|---|---|
| | $H_2O$ (average) | EG (average) | | |
| PBDB-T | 103.4 | 73.5 | 29.54 | —— |
| ETC-0F | 94.9 | 61.0 | 37.00 | 0.42 |
| ETC-1F | 95.4 | 62.0 | 36.17 | 0.34 |
| ETC-3F | 96.6 | 64.4 | 34.16 | 0.17 |

**Materials synthesis and characterization**

All chemicals, unless otherwise specified, were purchased from Aldrich or other commercial resources and used as received. Toluene was distilled from sodium benzophenone under nitrogen before using.

$^1$H and $^{13}$C NMR spectra were recorded on Bruker AV-400 MHz NMR spectrometer or Bruker AV-600 MHz NMR spectrometer. Chemical shifts are reported in parts per million (ppm, δ). $^1$H NMR and $^{13}$C NMR spectra were referenced to tetramethylsilane (0 ppm) for $CDCl_3$. Mass spectra were collected on a MALDI Micro MX mass spectrometer, or an API QSTAR XL System.

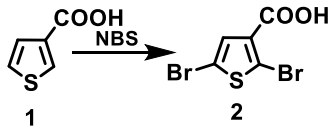


1 2

**2,5-dibromothiophene-3-carboxylic acid (2)**

In a Schlenk tube, thiophene-3-carboxylic acid (512.6 mg, 4 mmol) was dissolved in 8 ml N, N-Dimethylformamide, then N-Bromosuccinimide (1.78 g, 10 mmol) was added to the solution in batches under dark conditions. The reaction was stirred at 60 °C for 12 h and then the mixture was evacuated and filtered under reduced pressure with water to yield a white solid (1.12 g, 98%). $^1$H NMR (600 MHz, Chloroform-d): δ =7.41 (s,1H). $^{13}$C NMR (151 MHz, $CDCl_3$): δ = 165.14, 131.99, 130.80, 121.35, 111.72.

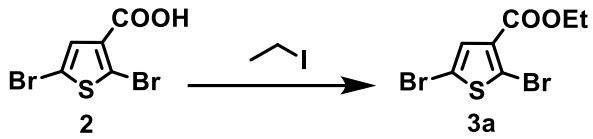


2 3a

**Ethyl 2,5-dibromothiophene-3-carboxylate (3a)**

To a Schlenk tube were added 2,5-dibromothiophene-3-carboxylic acid (300 mg, 1.05 mmol) and $K_2CO_3$ (578.2 mg, 4.19 mmol), and the mixture was subjected to three successive cycles of vacuum and nitrogen. Then, iodoethane (653.5 mg, 4.19 mmol) and dry DMF (6 ml) were added under the protection of nitrogen. The resulting mixture was stirred at 60 °C for 12 h. The crude product was extracted with dichloromethane and washed with saturated sodium chloride solution. After solvent removal, the product was purified using silica gel (petroleum ether/$CH_2Cl_2$, 1:1) to yield a white solid (294.5 mg, 90%). $^1$H NMR (600 MHz, Chloroform-d): δ = 7.33 (s, 1H), 4.31 (q, 2H), 1.36 (t, 3H). $^{13}$C NMR (151 MHz, $CDCl_3$): δ = 160.74, 131.88, 131.69, 119.07, 111.30, 61.28, 14.26.

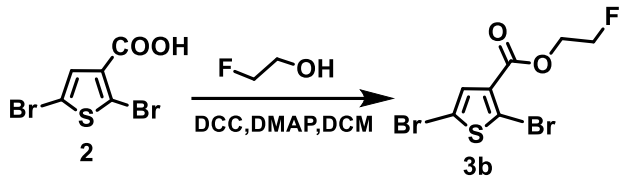


2 3b

**2-fluoroethyl 2,5-dibromothiophene-3-carboxylate (3b)**

To a Schlenk tube were added compound **2** (200 mg, 0.699 mmol), DCC (144.4mg, 0.699mmol) and DMAP (85.4 mg, 0.699mmol) and the mixture was subjected to three successive cycles of vacuum and nitrogen. Then, dry dichloroethane (6 ml) and 2-fluoroethan-1-ol (56.8 mg, 1.398 mmol) under the protection of nitrogen and the mixture was stirred for 24 h at 25 ℃. The crude product was extracted with dichloromethane and washed with saturated sodium chloride solution. After solvent removal, the product was purified using silica gel (petroleum ether/$CH_2Cl_2$, 1:1) to yield a white solid (171 mg, 74.67%). $^1$H NMR (600 MHz, Chloroform-*d*): δ = 7.39 (s, 1H), 4.73 (s, 1H), 4.67 (s, 1H), 4.54 (s, 1H), 4.48 (s, 1H). $^{13}$C NMR (151 MHz, $CDCl_3$): δ = 160.45, 131.65, 131.07, 120.02, 111.60, 81.68, 80.54, 64.05, 63.92.

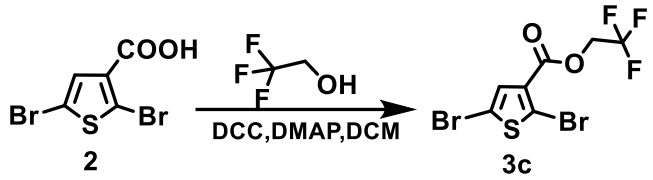


**2,2,2-trifluoroethyl 2,5-dibromothiophene-3-carboxylate (3c)**

To a Schlenk tube were added compound **2** (200 mg, 0.699 mmol), DCC (144.4mg, 0.699mmol) and DMAC (85.4 mg, 0.699 mmol) and the mixture was subjected to three successive cycles of vacuum and nitrogen. Then, dry dichloroethane (6 ml) and 2,2,2-trifluoroethan-1-ol (209.78 mg, 2.097 mmol) under the protection of nitrogen and the mixture was stirred for 24 h at 25 ℃. The crude product was extracted with dichloromethane and washed with saturated sodium chloride solution. After solvent removal, the product was purified using silica gel (petroleum ether/$CH_2Cl_2$, 9:1) to yield a white solid (135 mg, 53%). $^1$H NMR (600 MHz, Chloroform-*d*): δ = 7.38 (s, 1H), 4.63 (q, 2H). $^{13}$C NMR (151 MHz, $CDCl_3$): δ = 158.87, 131.48, 129.83, 123.76, 121.92, 121.38, 112.03, 61.09, 60.84, 60.60, 60.35.

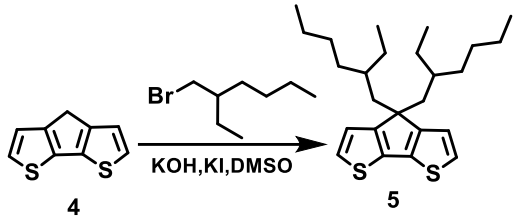


**4,4-bis(2-ethylhexyl)-4H-cyclopenta[2,1-b:3,4-b']dithiophene (5)**

4H-cyclopenta[2,1-b:3,4-b']dithiophene (1.78 g, 10 mmol), 2-ethylhexyl bromide (4 g, 21 mmol), KOH (1.84 g, 32.8 mmol) and KI (0.24 g, 1.4 mmol) were dissolved in 40 mL DMSO (dimethylsulfoxide) and stirred at 30 ºC overnight. Then the mixture was washed with water and extracted with diethyl ether. The combined organic phase was evaporated under vacuum and the obtained crude product was purified on silica gel column chromatography with hexane as the eluent, yielding a light-yellow liquid (3.0 g, 74%).$^1$H NMR (400 MHz, $CDCl_3$): δ = 7.04 (d, *J* = 4.9 Hz, 2H), 6.88-6.82 (m, 2H), 1.86-1.72 (m, 4H), 1.01-0.74 (m, 16H), 0.68 (t, *J* = 6.9 Hz, 6H), 0.51 (t, *J* = 7.5 Hz, 8H).

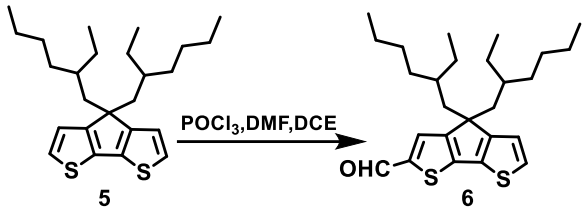


**4,4-bis(2-ethylhexyl)-4H-cyclopenta[2,1-b:3,4-b‘]dithiophene-2-carbaldehyde (6)**

Compound **5** (804 mg, 2 mmol) was dissolved in 10 mL dichloroethane under $N_2$ atmosphere, then the freshly prepared Vilsmeier reagent (0.2 mL $POCl_3$ into 0.4 mL DMF) was added dropwise at 0 °C. After stirring for 30 min at 0 °C, the mixture was heated to 80 °C and refulxed overnight. The reaction was quenched by saturated $K_2CO_3$ solution and allowed to stir at room temperature for 15 min. The mixture was extracted with diethyl ether for three times. The combined organic layer was washed with water and brine, dried over $Na_2SO_4$, and concentrated under reduced pressure. The crude product was purified by column chromatography (stationary phase: silica gel; eluent: n-hexane/DCM = 2:3) to get the product as an orange oil (740 mg, 86%). $^1$H NMR (400 MHz, $CDCl_3$): δ = 9.83 (s, 1H), 7.57 (s, 1H), 7.38 (s, 1H), 7.01 (s, 1H), 1.93 (s, 4H), 1.60 (s, 2H), 1.09-0.81 (m, 20H), 0.60 (d, *J* = 12.0 Hz, 8H).

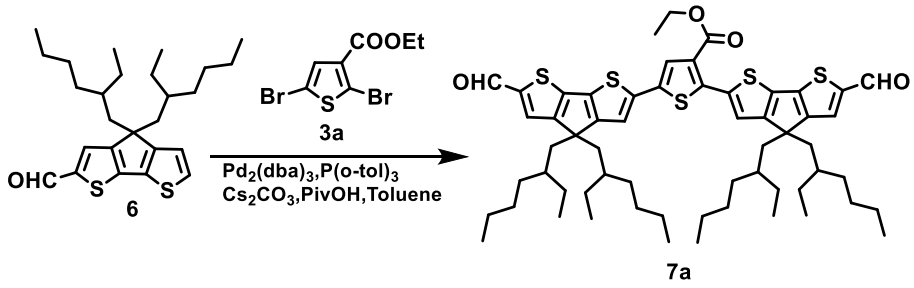


**Ethyl 2,5-bis(4,4-bis(2-ethylhexyl)-6-formyl-4H-cyclopenta[2,1-b:3,4-b']dithiophen-2-yl)thiophene-3-carboxylate (7a)**

To a Schlenk tube were added compound **6** (297 mg, 0.675 mmol), compound **3a** (100 mg, 0.27 mmol), $Cs_2CO_3$ (263.9 mg, 0.81 mmol), and trimethylacetic acid (11.0 mg, 0.108 mmol). $Pd_2(dba)_3$ (12.4 mg, 0.0135 mmol) and P(o-tol)$_3$ (9.5 mg , 0.027 mmol) were added, and the mixture was subjected to three successive cycles of vacuum and nitrogen. Dry toluene (6 ml) was added, and the tube was sealed and heated at 110 ℃

for only 1 h. The crude product was extracted with dichloromethane and washed with saturated sodium chloride solution. After solvent removal, the product was purified using silica gel (petroleum ether/$CH_2Cl_2$, 1:1) to yield an orange-red product (177.9 mg , 65%). $^1$H NMR (600 MHz, Chloroform-*d*): δ 9.85 (s, 2H), 7.58 (q, *J* = 5.4 Hz, 3H), 7.54 – 7.43 (m, 1H), 7.15 - 7.02 (m, 1H), 4.37 (q, 2H), 1.93 (m, 8H), 1.40 (t, 3H), 1.01 - 0.86 (m, 32H), 0.76 – 0.74 (m, 12H), 0.65 – 0.61 (m, 16H). $^{13}$C NMR (151 MHz, $CDCl_3$): δ = 182.52, 171.16, 162.54, 161.27, 158.20, 147.29, 147.16, 143.58, 142.16, 139.49, 139.47, 139.11, 137.37, 135.77, 135.01, 134.98, 130.56, 127.88, 126.57, 124.39, 119.59, 61.20, 54.31, 43.05, 35.30, 34.20, 28.56, 27.33, 22.76, 14.38, 14.08, 10.71, 10.62.

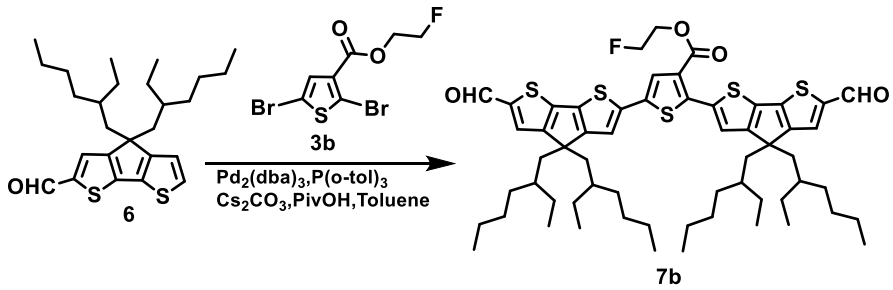


**2-fluoroethyl 2,5-bis(4,4-bis(2-ethylhexyl)-6-formyl-4H-cyclopenta[2,1-b:3,4-b']dithiophen-2-yl)thiophene-3-carboxylate (7b)**

This compound was prepared following the same procedure as for compound 7a. The product was afforded as a dark blue solid (178.2 mg, 64%). $^1$H NMR (600 MHz, Chloroform-*d*): δ = 9.85 (s, 2H), 7.62 (t, *J* = 2.8 Hz, 1H), 7.59 (t, *J* = 5.8 Hz, 2H), 7.51 (d, *J* = 8.6 Hz, 1H), 7.14 - 7.12 (m, 1H), 4.78 (s, 1H), 4.70 (s, 1H), 4.60 (s, 1H), 4.54 (s, 1H), 1.99 – 1.92 (m, 8H), 1.00 – 0.92 (m, 32H), 0.77 – 0.75 (m, 12H), 0.65 – 0.63 (m, 16H). $^{13}$C NMR (151 MHz, $CDCl_3$): δ = 182.52, 162.60, 162.29, 161.41, 158.30, 157.80, 147.16, 144.01, 143.64, 142.99, 139.28, 137.05, 135.93, 135.15, 130.57, 126.50, 124.61, 119.66, 114.07, 81.82, 80.69, 64.00, 54.27, 43.04, 37.11, 35.30, 34.20, 31.94, 27.34, 22.76, 19.74, 14.15, 10.62.

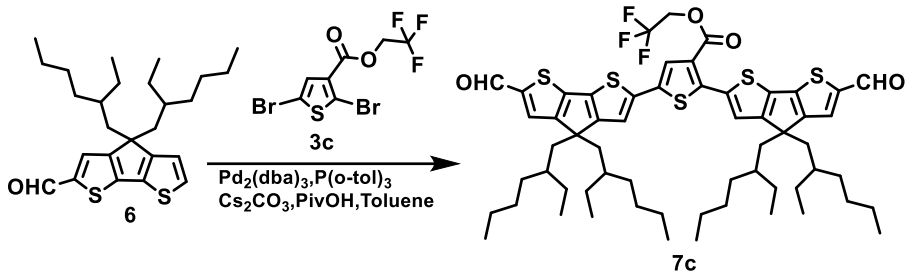


**2,2,2-trifluoroethyl 2,5-bis(4,4-bis(2-ethylhexyl)-6-formyl-4H-cyclopenta[2,1-b:3,4-b']dithiophen-2-yl)thiophene-3-carboxylate (7c)**

This compound was prepared following the same procedure as for compound 7a. The product was afforded as a dark blue solid (172.9 mg, 60%). $^{1}$H NMR (600 MHz, Chloroform-*d*): δ = 9.86 (s, 2H), 7.59 (m, 3H), 7.55 (m, 1H), 7.13 (m, 1H), 4.69 (q, *J* = 8.3 Hz, 2H), 2.0 – 1.92 (m, 8H), 1.00 – 0.92 (m, 32H), 0.76 – 0.74 (m, *J* = 7.2 Hz, 12H), 0.63 – 0.62 (m, 16H). $^{13}$C NMR (151 MHz, $CDCl_3$): δ = 182.56, 162.57, 161.52, 160.61, 158.42, 157.88, 146.99, 144.18, 143.74, 139.39, 138.90, 136.49, 136.14, 130.64, 126.12, 124.91, 123.90, 122.06, 119.85, 60.71, 60.46, 54.33, 43.04, 35.30, 34.10, 31.44, 30.19, 29.71, 28.56, 27.33, 22.75, 14.07, 10.61.

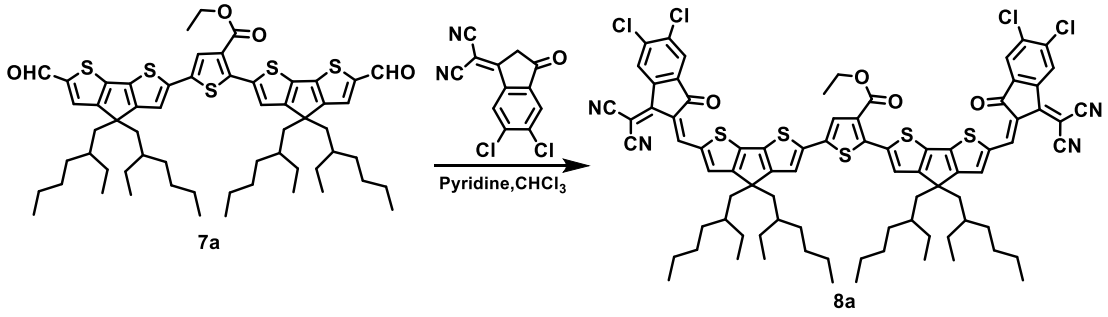


**Ethyl 2,5-bis(6-(((Z)-5,6-dichloro-1-(dicyanomethylene)-3-oxo-1,3-dihydro-2H-inden-2-ylidene)methyl)-4,4-bis(2-ethylhexyl)-4H-cyclopenta[2,1-b:3,4-b']dithiophen-2-yl)thiophene-3-carboxylate (8a)**

To a Schlenk tube were added 2-(5,6-dichloro-3-oxo-2,3-dihydro-1H-inden-1-ylidene)malononitrile (52.6 mg, 0.2mmol) and the mixture was subjected to three successive cycles of vacuum and nitrogen. Then, compound **6a** (50.9mg, 0.05 mmol), dry pyridine (0.5ml) and dry $CHCl_3$ (5 ml) were added under the protection of nitrogen.The resulting mixture was stirred at 25 °C for 2 h. The crude product was extracted with dichloromethane and washed with saturated sodium chloride solution.

After solvent removal, the product was purified using silica gel (petroleum ether/$CH_2Cl_2$, 1:1) to yield dark blue solid (53.2 mg , 74%). $^1$H NMR (600 MHz, Chloroform-*d*): δ = 8.92 (s, 2H), 8.74 (s, 2H), 7.92 (d, 2H), 7.68 (t, 2H), 7.61 (m, 2H), 7.18 (m, 1H), 4.43 (q, 2H), 2.05 – 1.97 (q, 8H), 1.45 – 1.43 (t, 3H),1.01 - 0.94 (m, 32H), 0.76 - 0.63 (m, 16H), 0.67 - 0.63 (q, 12H). $^{13}$C NMR (151 MHz, $CDCl_3$): δ = 186.26, 166.39, 164.87, 162.46, 158.35, 143.45, 142.20, 141.31, 139.79, 139.48, 139.32, 139.07, 138.65, 136.68, 136.05, 127.96, 126.83, 124.98, 124.92, 124.77, 124.63, 119.81, 114.61, 68.39, 61.53, 54.19, 43.14, 35.54, 35.49, 34.29, 34.20, 34.10, 34.01, 28.49, 27.49, 27.31, 22.82, 14.42, 14.11, 10.63.

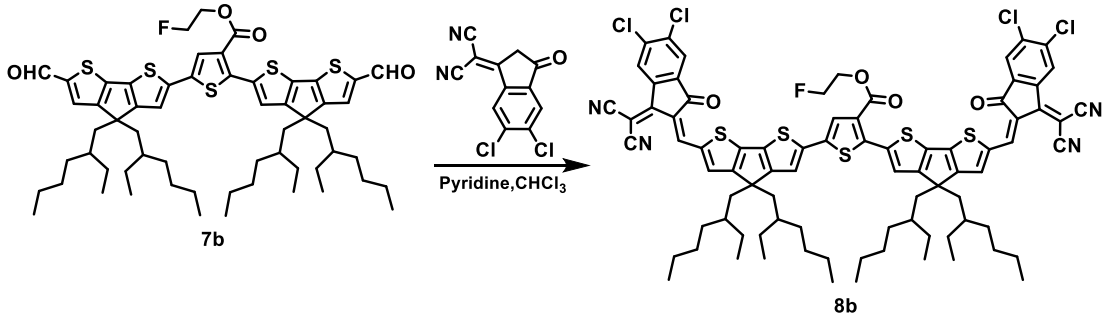


**2-fluoroethyl 2,5-bis(6-(((Z)-5,6-dichloro-1-(dicyanomethylene)-3-oxo-1,3-dihydro-2H-inden-2-ylidene)methyl)-4,4-bis(2-ethylhexyl)-4H-cyclopenta[2,1-b:3,4-b']dithiophen-2-yl)thiophene-3-carboxylate (8b)**

This compound was prepared following the same procedure as for compound 7a. The product was afforded as a dark blue solid (81.6 mg, 71.3%). $^1$H NMR (600 MHz, Chloroform-d): δ = 8.92 (s, 2H), 8.74 (s, 2H), 7.93 (d, 2H), 7.72 (t, J = 52.7 Hz, 2H), 7.63 (m, 2H), 4.82 (t, 1H), 4.74 (t, 1H), 4.64 (t, 1H), 4.59 (t, 1H), 2.03 – 1.98 (m, 8H), 1.02 – 0.94 (s, 32H), 0.76 - 0.72 (s, 16H), 0.67 - 0.65 (m, 12H). $^{13}$C NMR (151 MHz, $CDCl_3$): δ = 186.06, 166.38, 164.98, 162.04, 160.06, 159.61, 158.23, 143.21, 142.98, 140.95, 139.87, 139.54, 139.34, 139.10, 138.62, 138.40, 136.78, 136.01, 135.41, 127.83, 126.81, 124.97, 119.82, 119.62, 114.56, 81.80, 80.66, 68.44, 68.29, 64.26, 64.12, 54.24, 43.19, 35.53, 35.48, 34.28, 34.18, 34.10, 34.02, 28.44, 27.47, 27.32, 22.84, 14.12, 10.63.

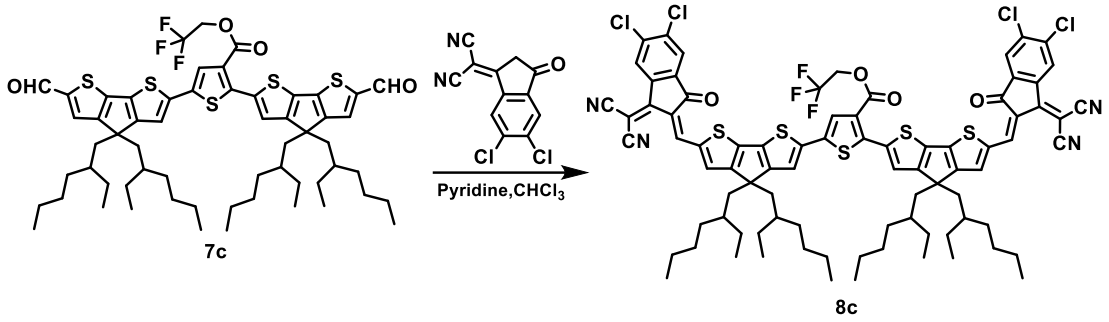


**2,2,2-trifluoroethyl 2,5-bis(6-(((Z)-5,6-dichloro-1-(dicyanomethylene)-3-oxo-1,3-dihydro-2H-inden-2-ylidene)methyl)-4,4-bis(2-ethylhexyl)-4H-cyclopenta[2,1-b:3,4-b']dithiophen-2-yl)thiophene-3-carboxylate (7c)**

This compound was prepared following the same procedure as for compound 7a. The product was afforded as a dark blue solid (88.5 mg, 76.5%). $^{1}$H NMR (600 MHz, Chloroform-*d*): δ = 8.94 (s, 2H), 8.76 (s, 2H), 7.93 (d, 2H), 7.70 (t, 2H), 7.63 (m, 2H), 7.21 (m, 1H), 4.73 (q, 2H), 2.03 – 1.96 (m, 8H), 1.02 – 0.94 (m, 32H), 0.75 -0.70 (m, 16H), 0.66 -0.63 (m, 12H). $^{13}$C NMR (151 MHz, $CDCl_3$): δ = 186.13, 166.30, 165.02, 160.41, 160.09, 158.19, 144.19, 142.72, 140.24, 139.97, 139.61, 139.41, 139.36, 139.17, 139.10, 138.40, 136.96, 136.00, 135.71, 127.36, 126.83, 124.92, 122.02, 120.02, 119.71, 114.54, 77.28, 68.41, 60.87, 54.30, 43.19, 35.53, 34.26, 34.21, 34.10, 34.01, 28.52, 28.49, 28.44, 27.46, 27.32, 22.84, 14.12, 10.62, 10.57.

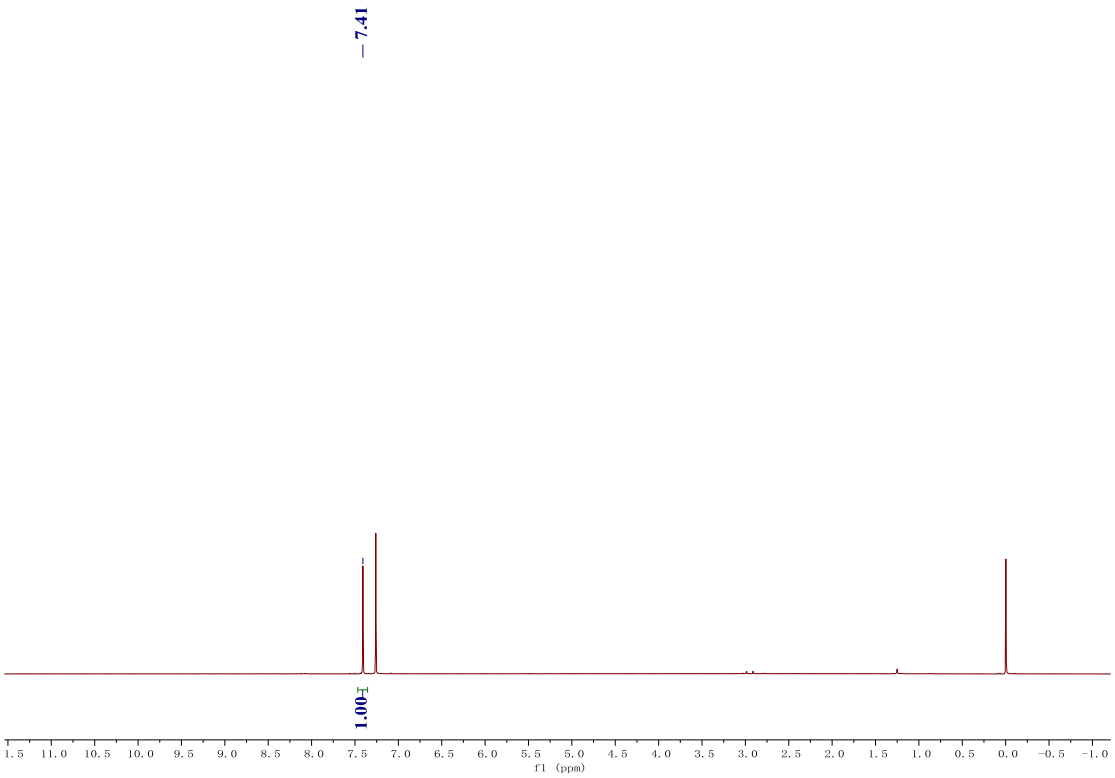


**Figure S10.** $^{1}$H NMR spectrum of compound 2.

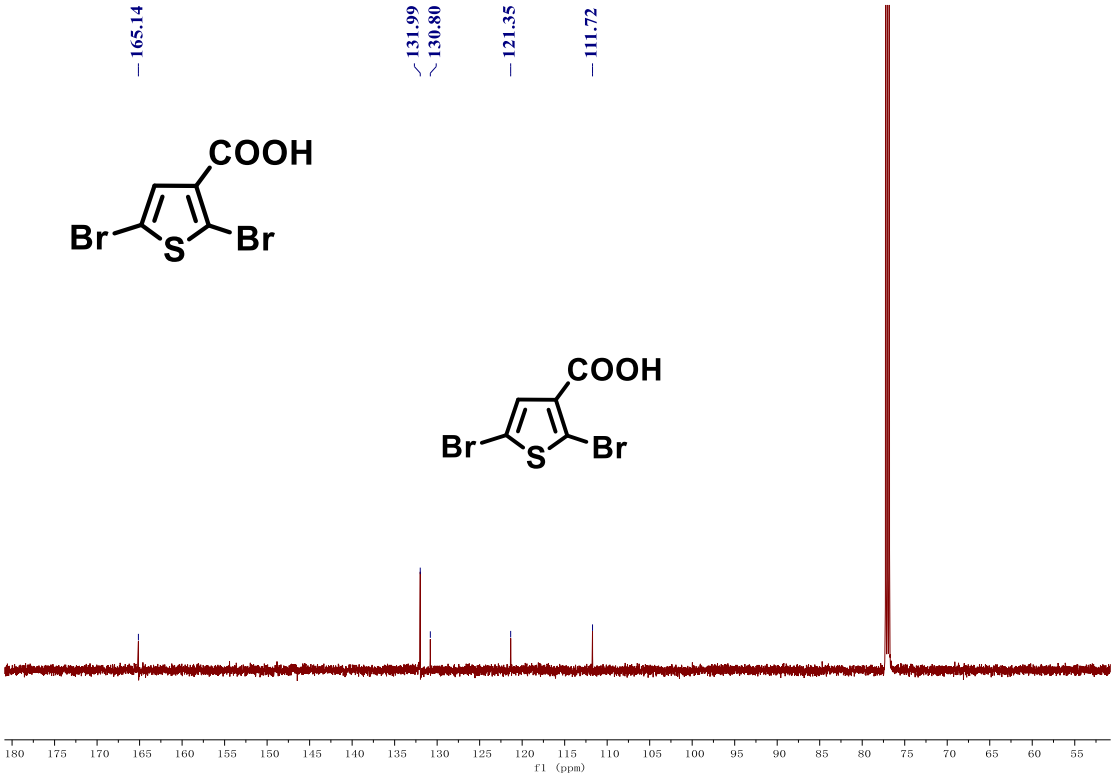


**Figure S11.** $^{13}$C NMR spectrum of compound 2.

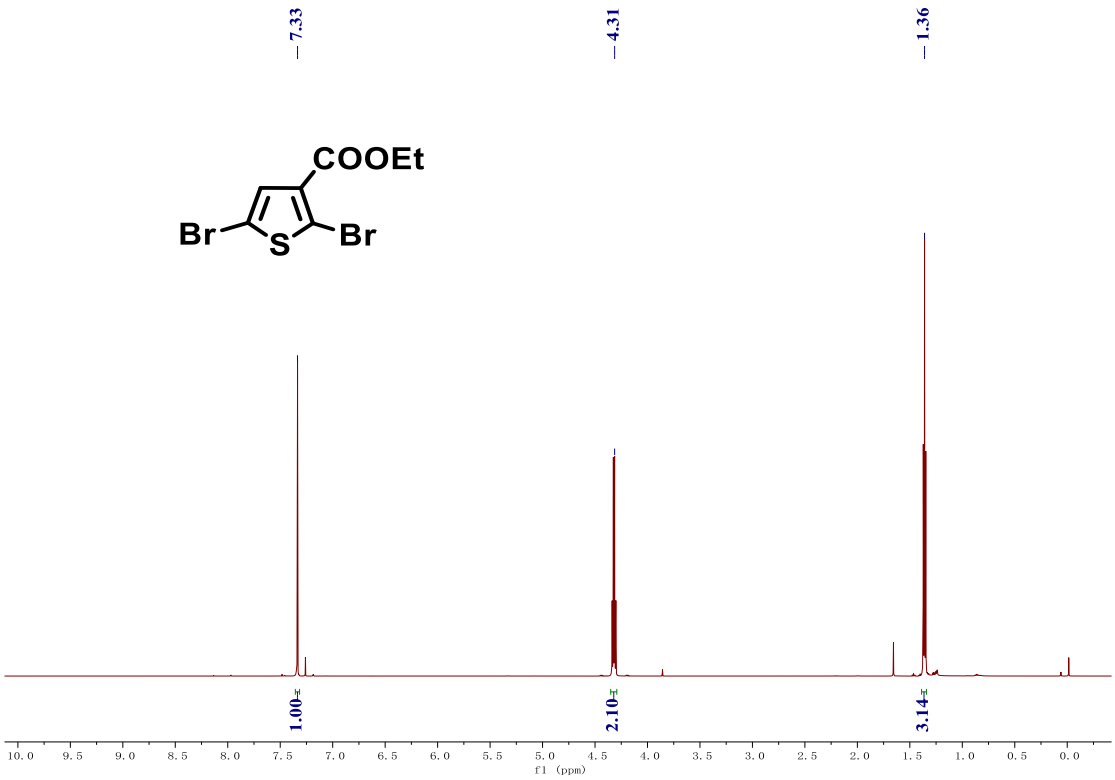


**Figure S12.** $^{1}$H NMR spectrum of compound 3a.

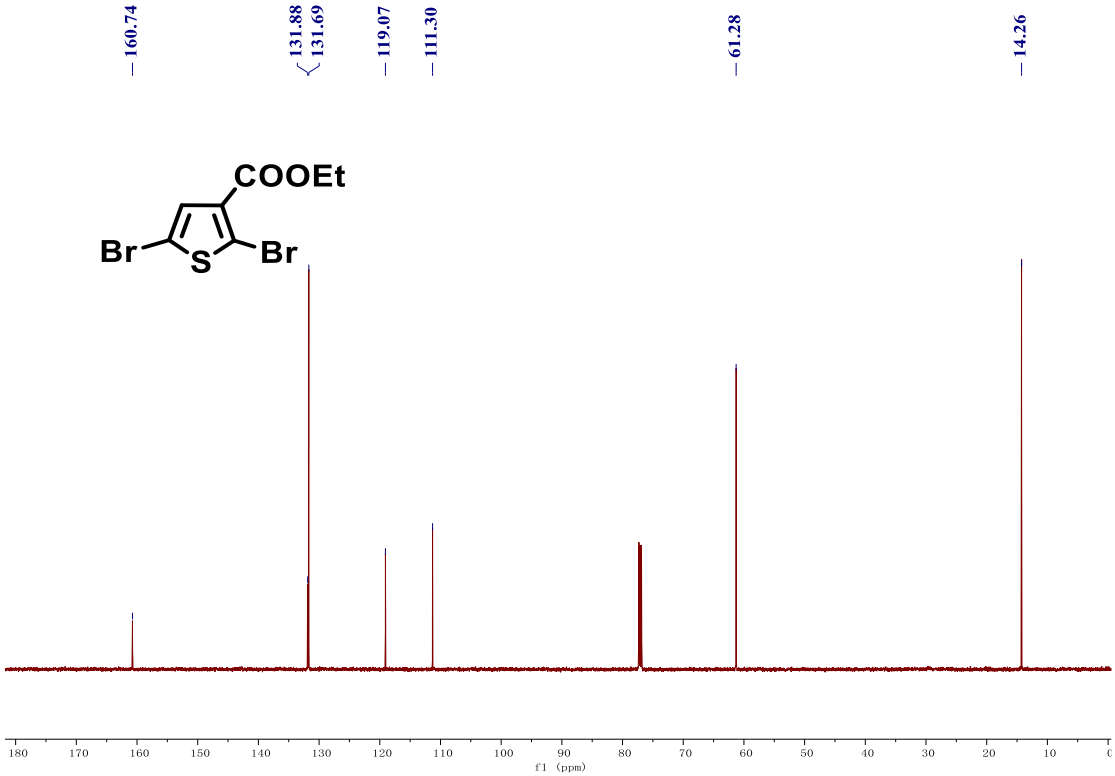


**Figure S13.** $^{13}$C NMR spectrum of compound 3a.

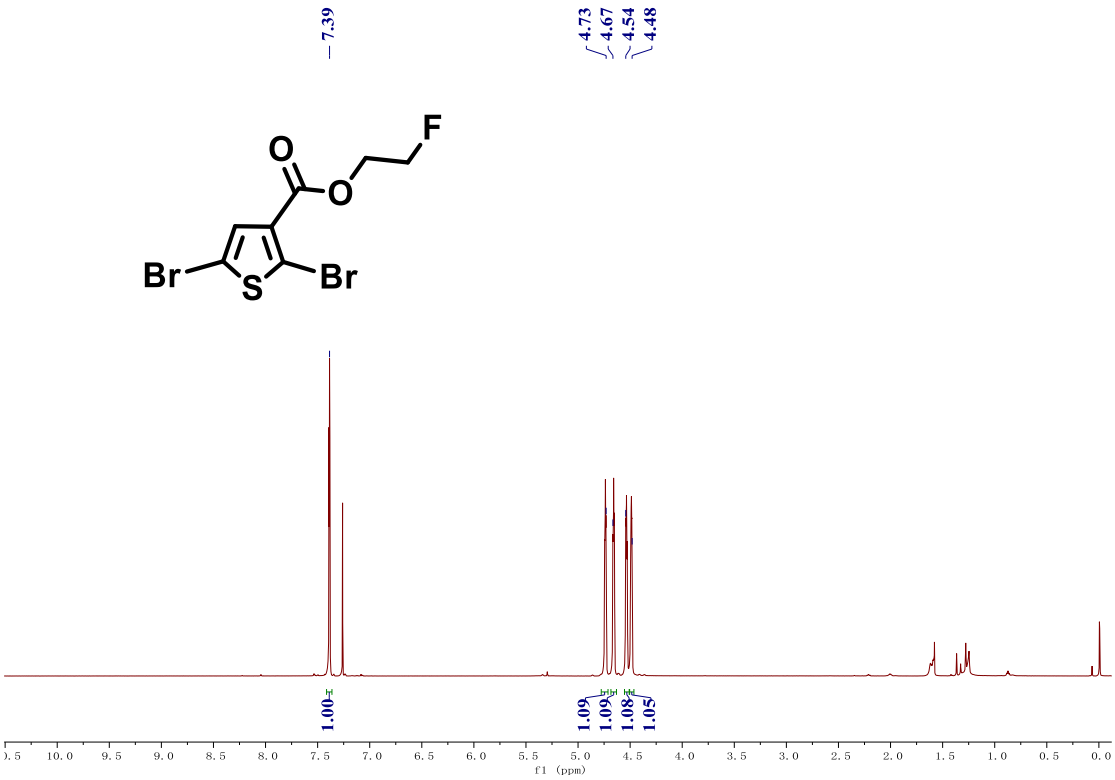


**Figure S14.** $^{1}$H NMR spectrum of compound 3b.

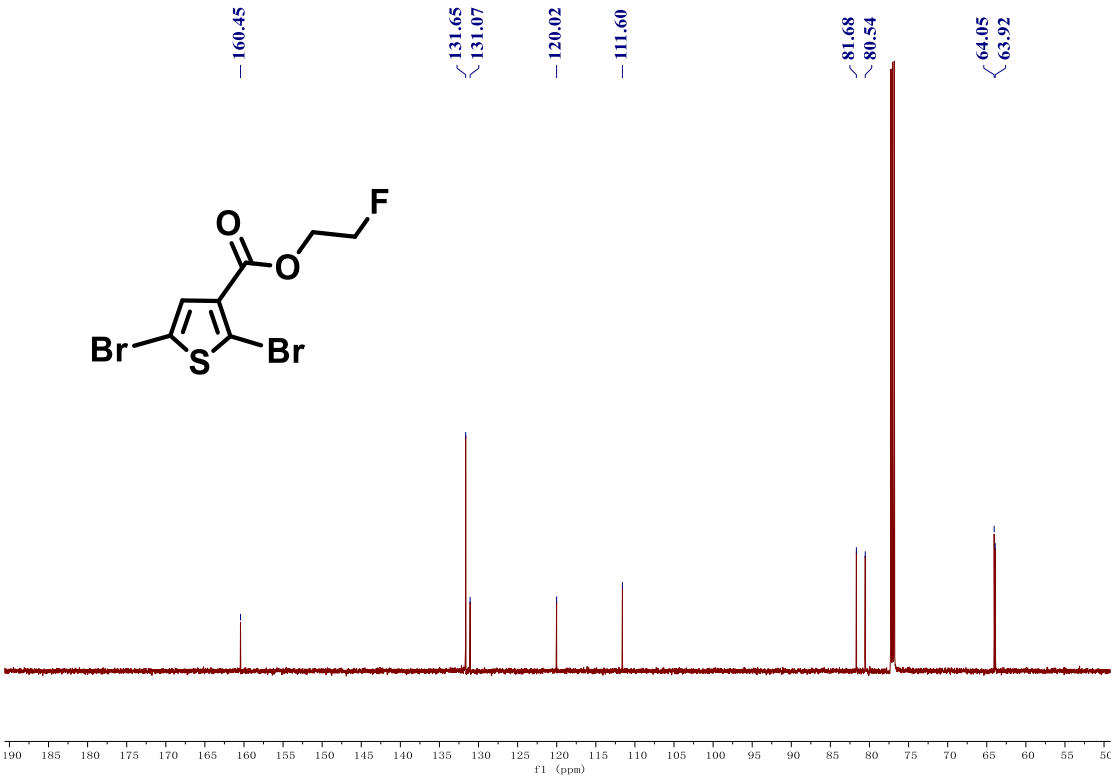


**Figure S15.** $^{13}$C NMR spectrum of compound 3b.

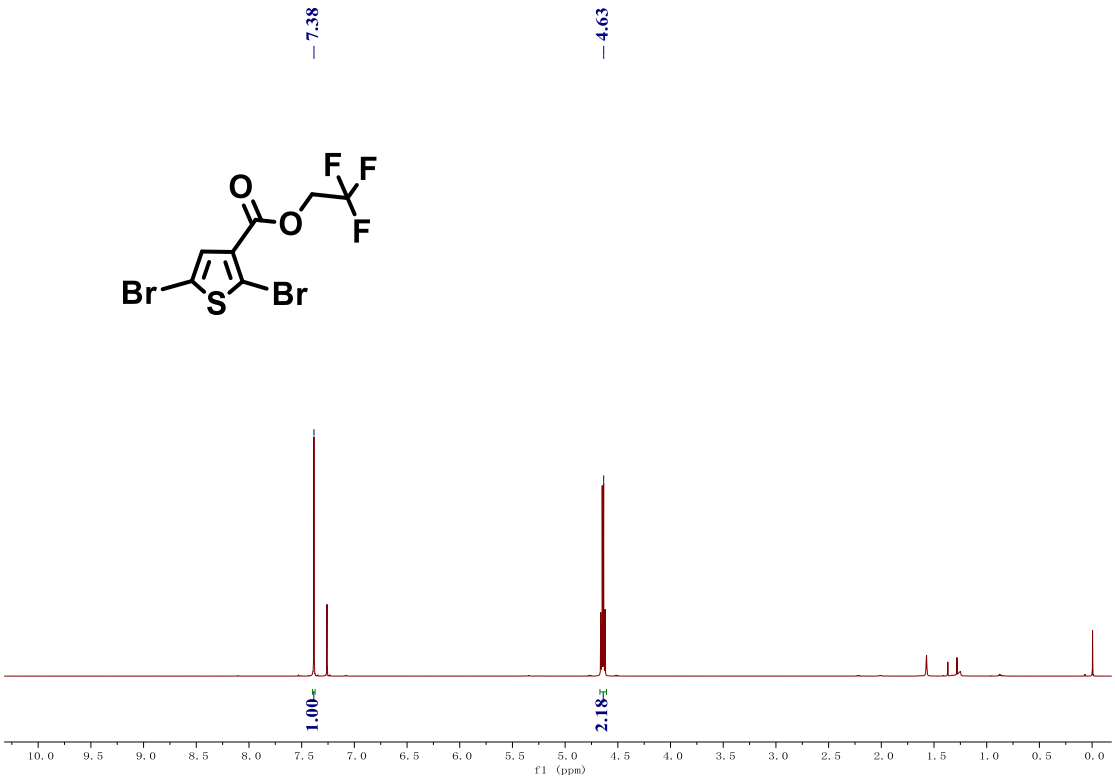


**Figure S16.** $^{1}$H NMR spectrum of compound 3c.

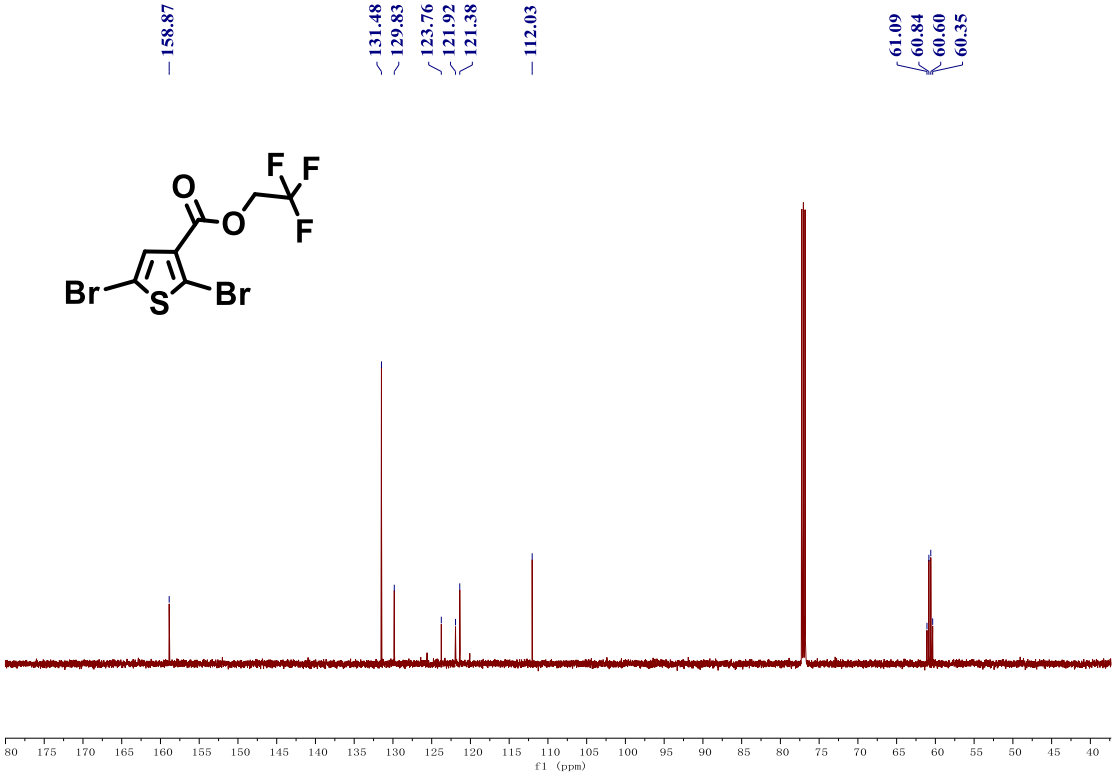


**Figure S17.** $^{13}$C NMR spectrum of compound 3c.

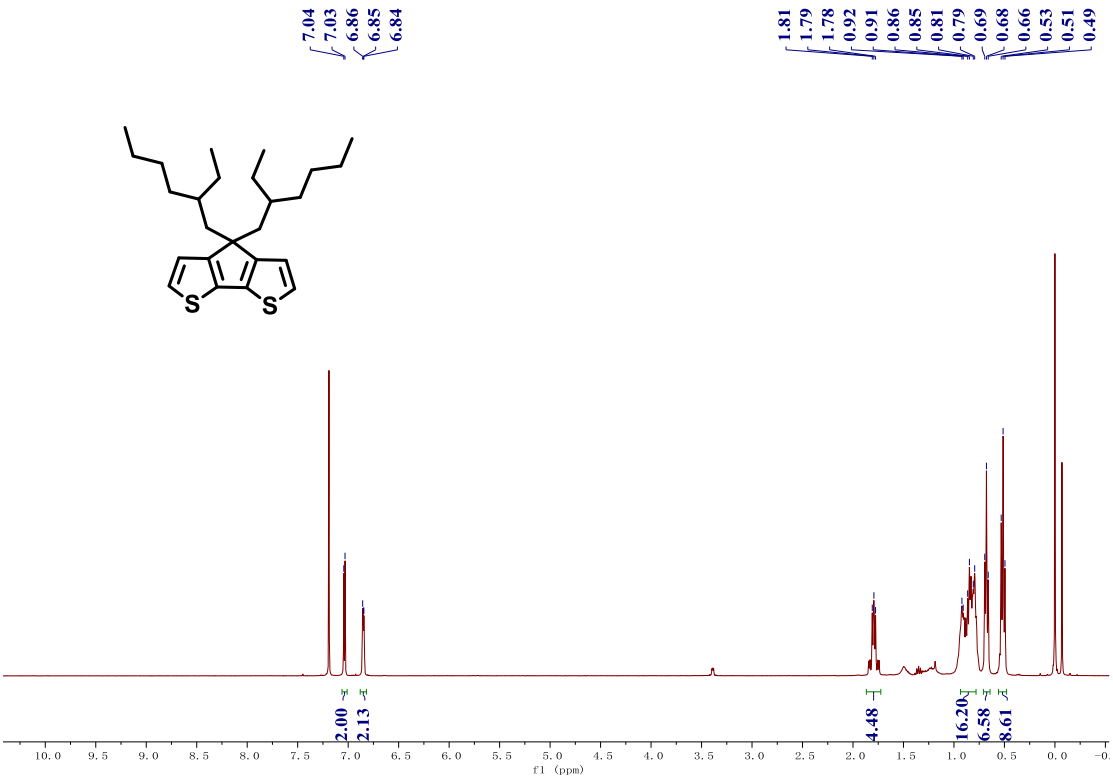


**Figure S18.** $^{1}$H NMR spectrum of compound 5.

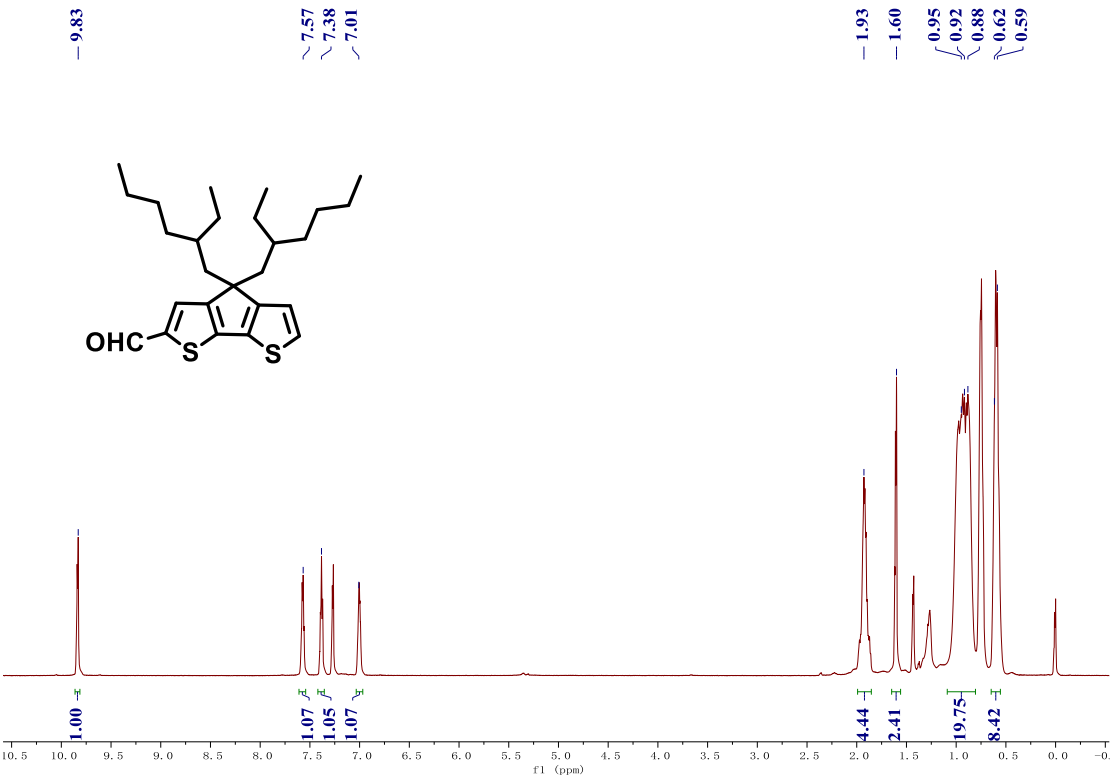


**Figure S19.** $^{1}$H NMR spectrum of compound 6.

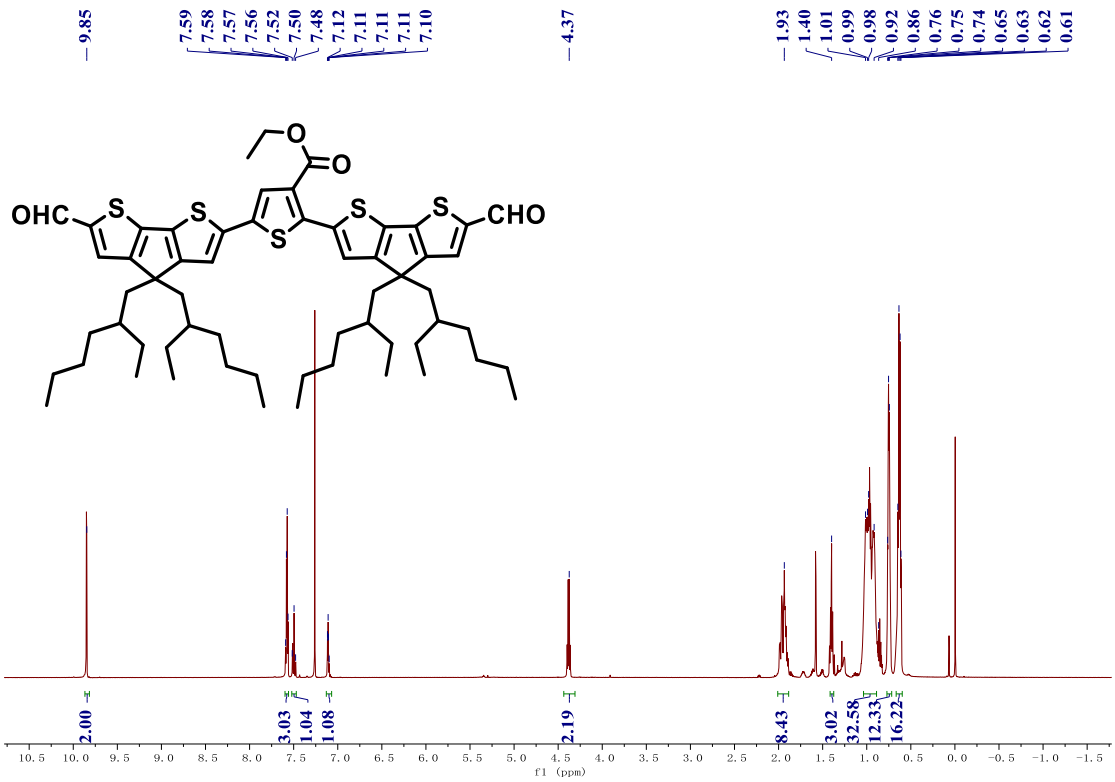


**Figure S20.** $^{1}$H NMR spectrum of compound 7a.

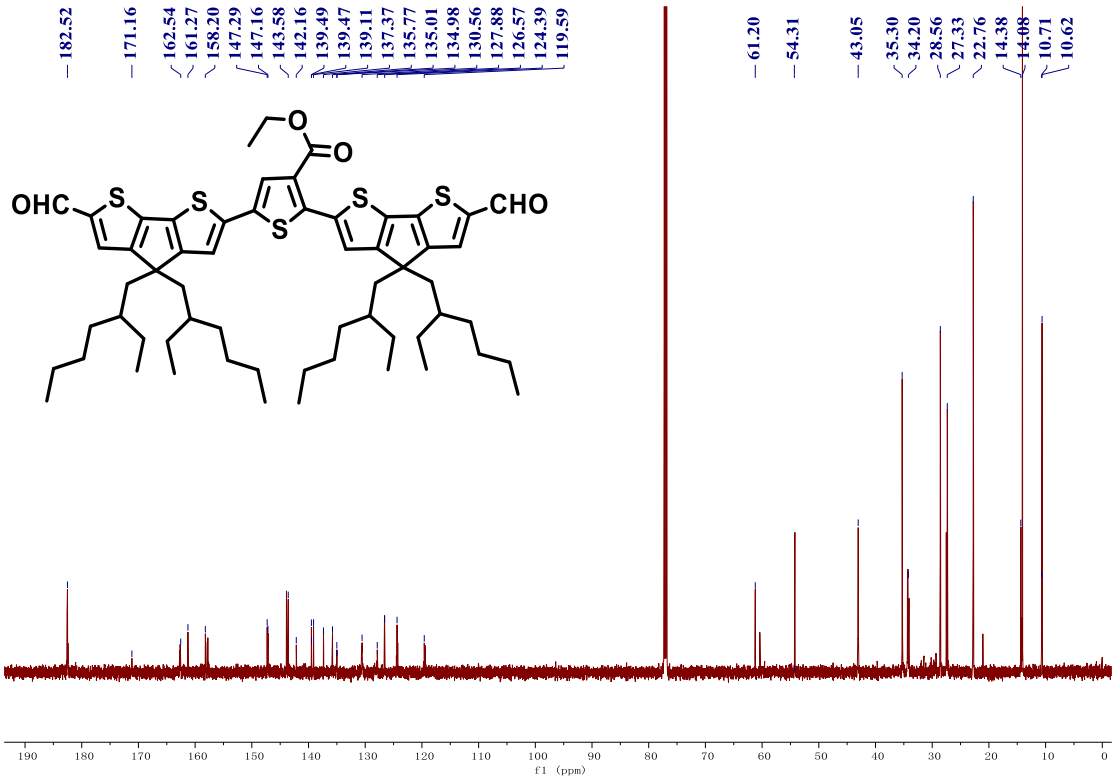


**Figure S21.** $^{13}$C NMR spectrum of compound 7a.

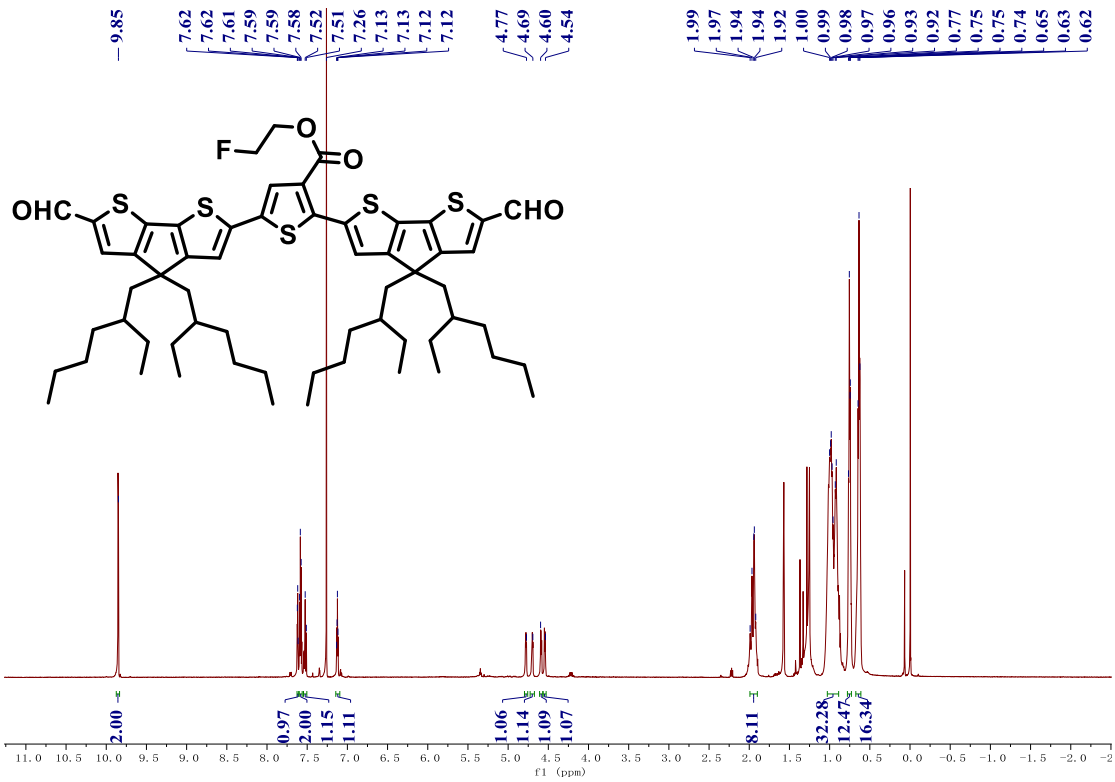


**Figure S22.** $^{1}$H NMR spectrum of compound 7b.

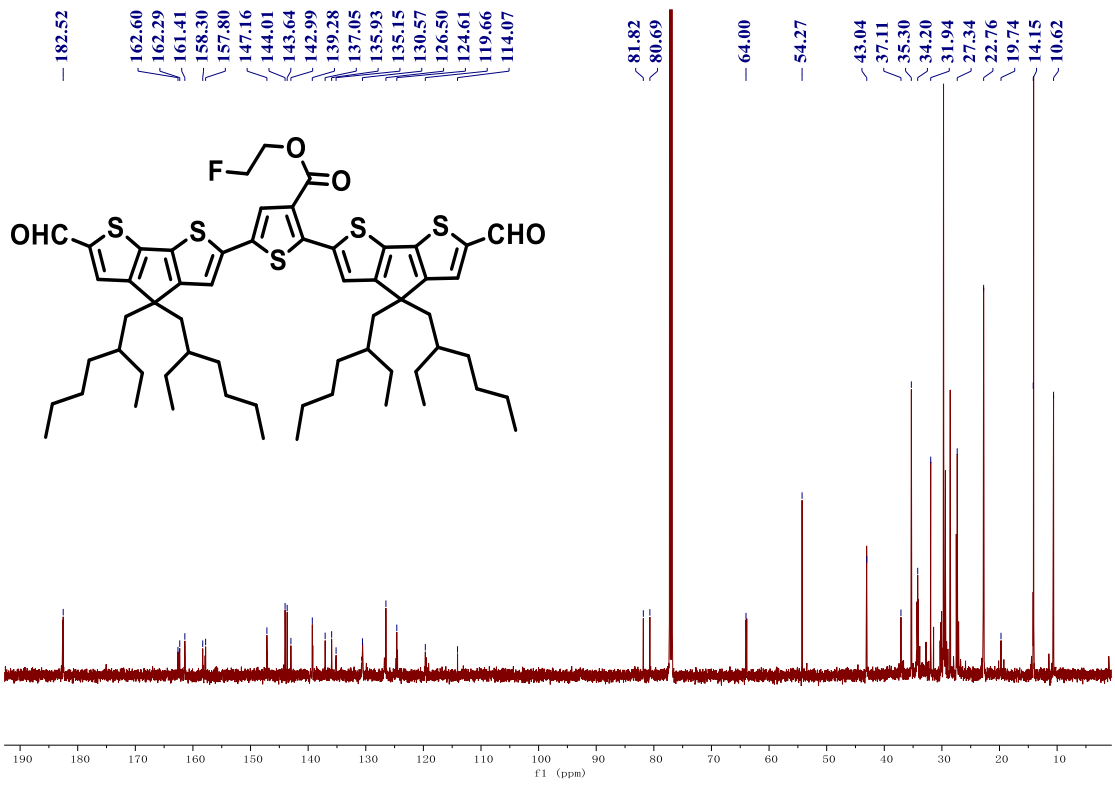


**Figure S23.** $^{13}$C NMR spectrum of compound 7b.

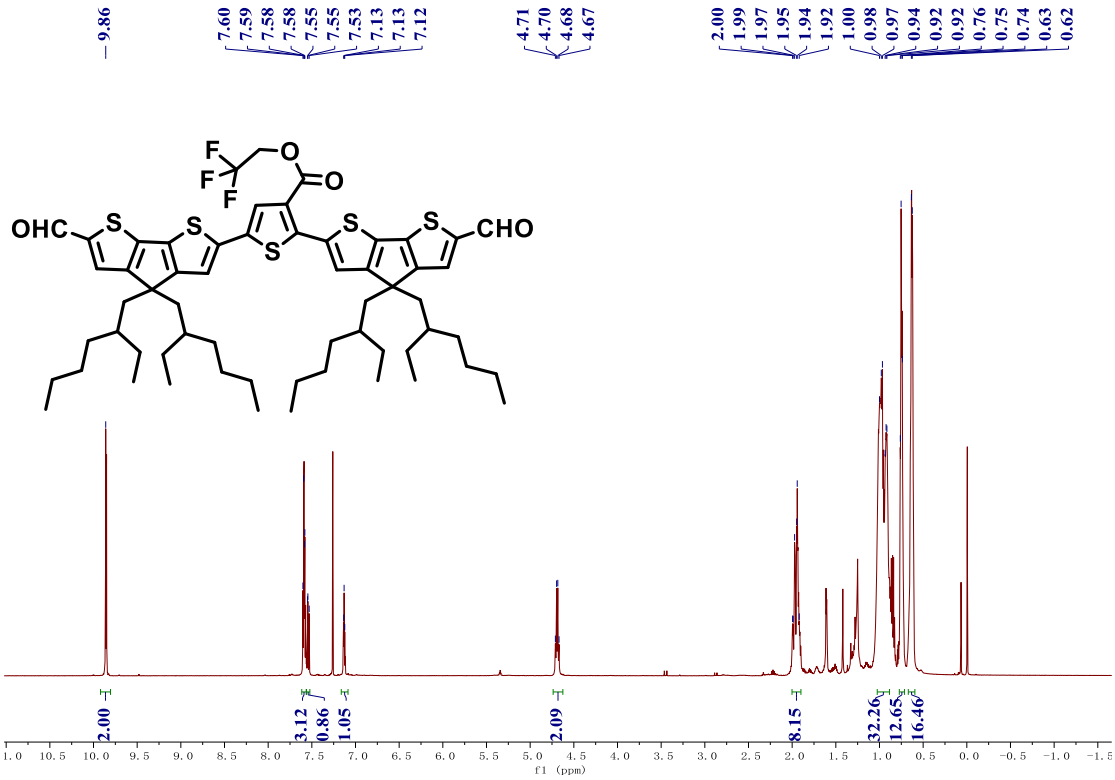


**Figure S24.** $^{1}$H NMR spectrum of compound 7c.

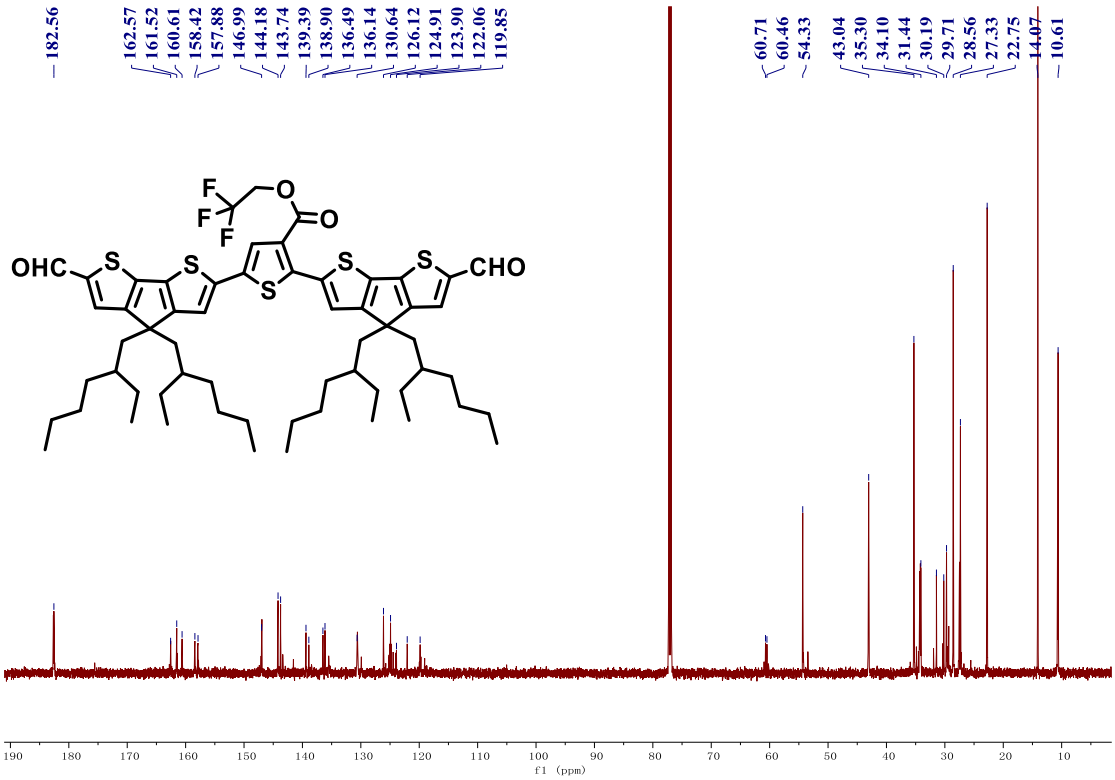


**Figure S25.** $^{13}$C NMR spectrum of compound 7c.

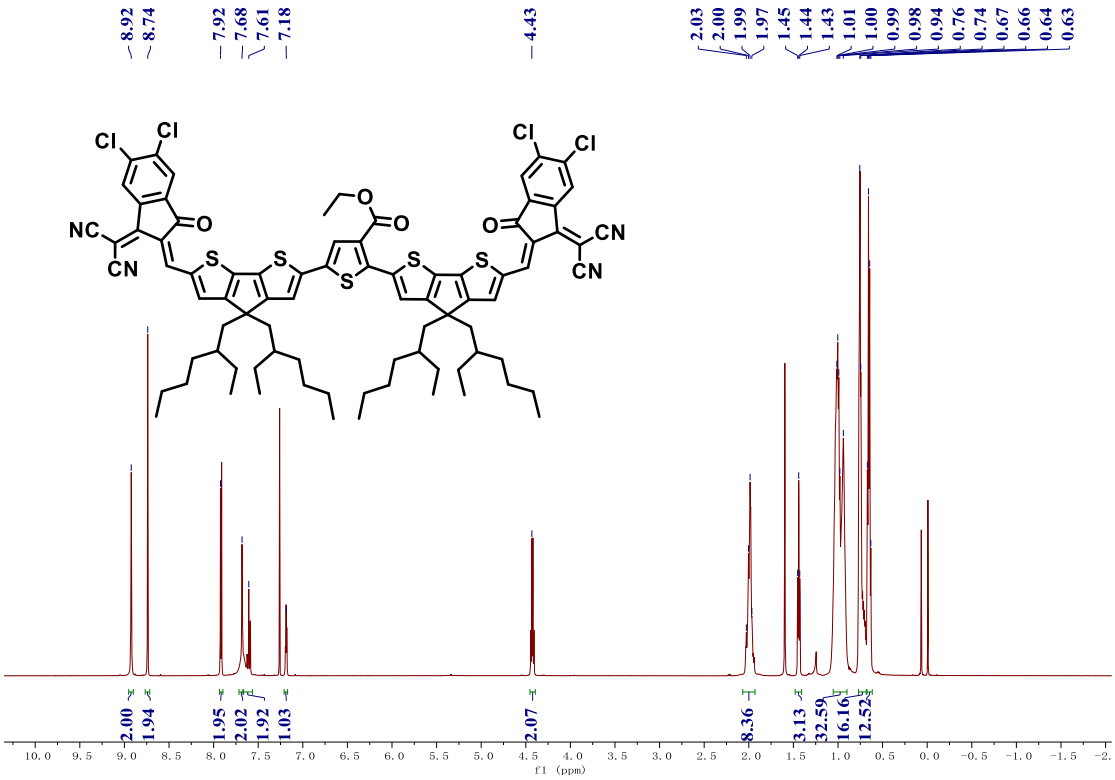


**Figure S26.** $^{1}$H NMR spectrum of compound 8a.

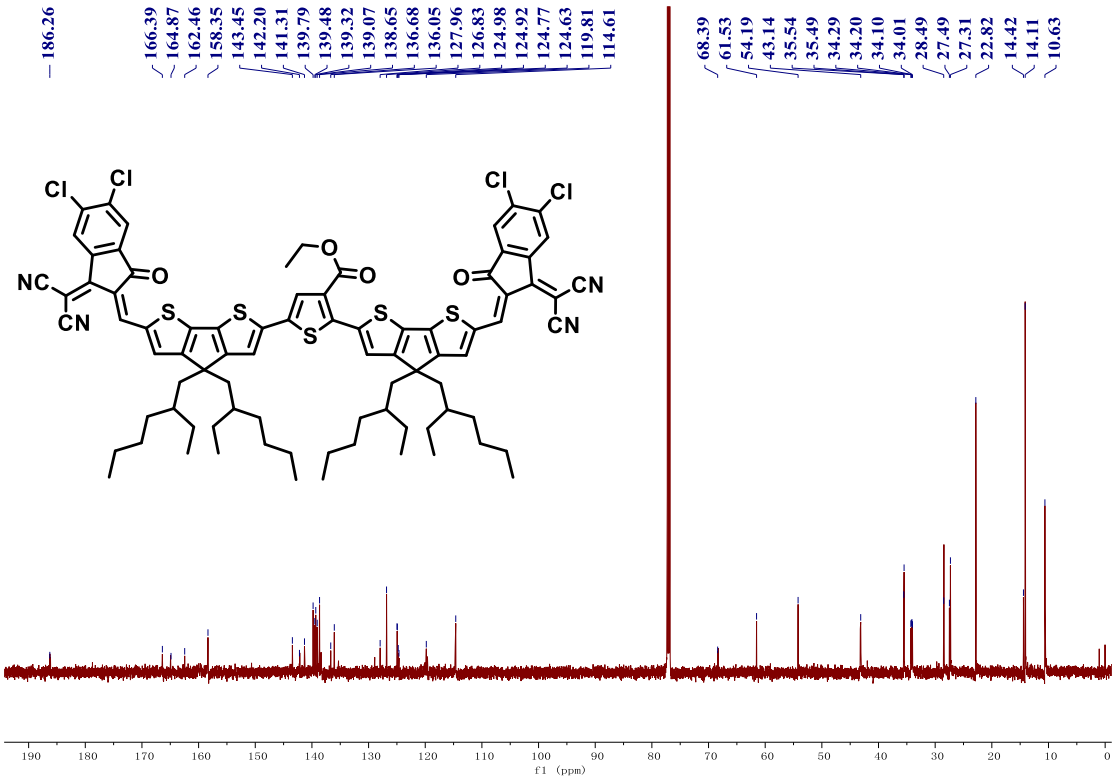


**Figure S27.** $^{13}$C NMR spectrum of compound 8a.

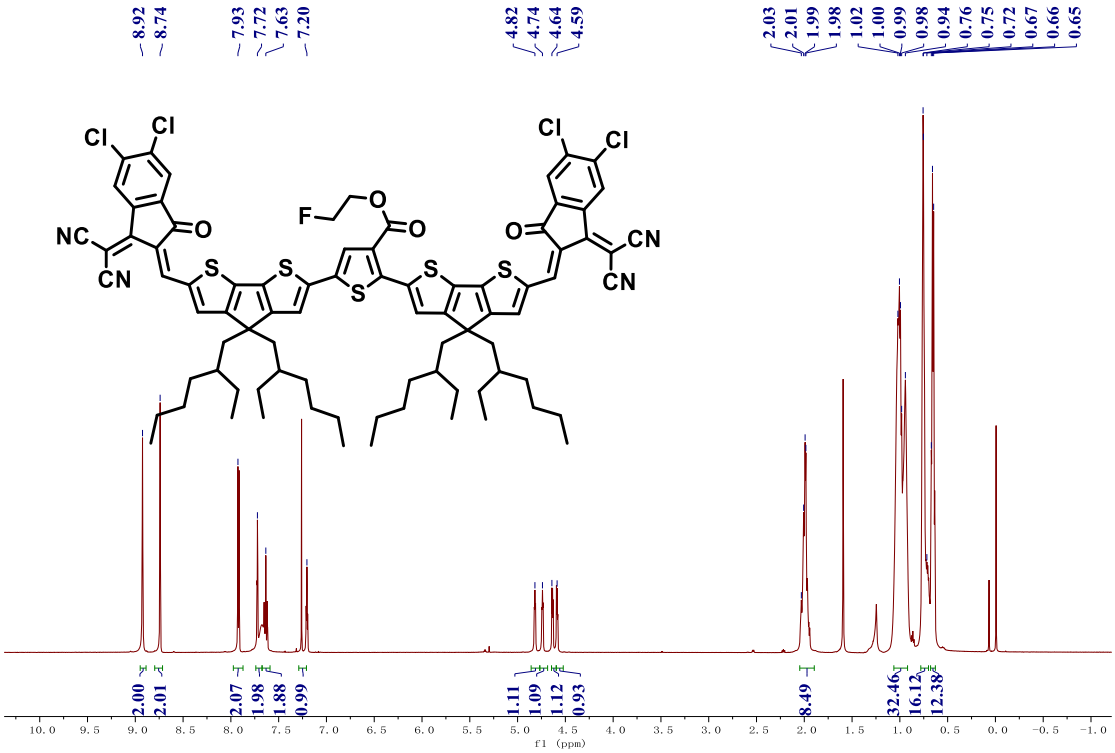


**Figure S28.** $^{1}$H NMR spectrum of compound 8b.

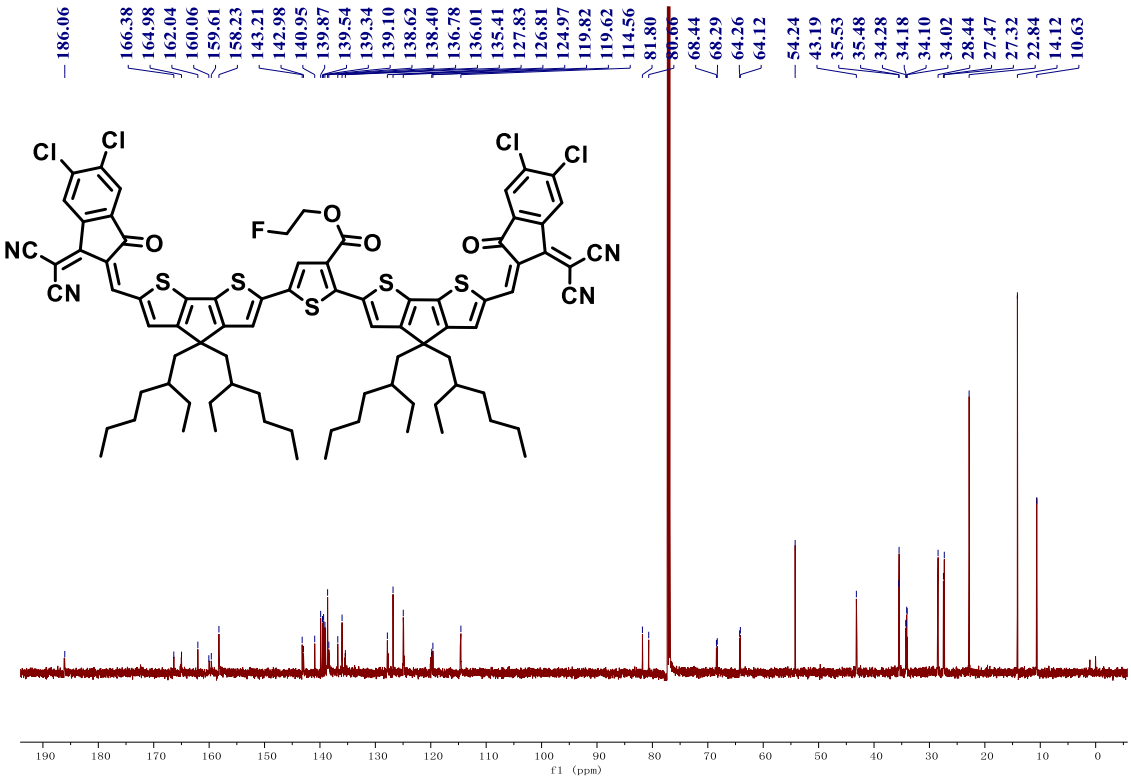


**Figure S29.** $^{13}$C NMR spectrum of compound 8b.

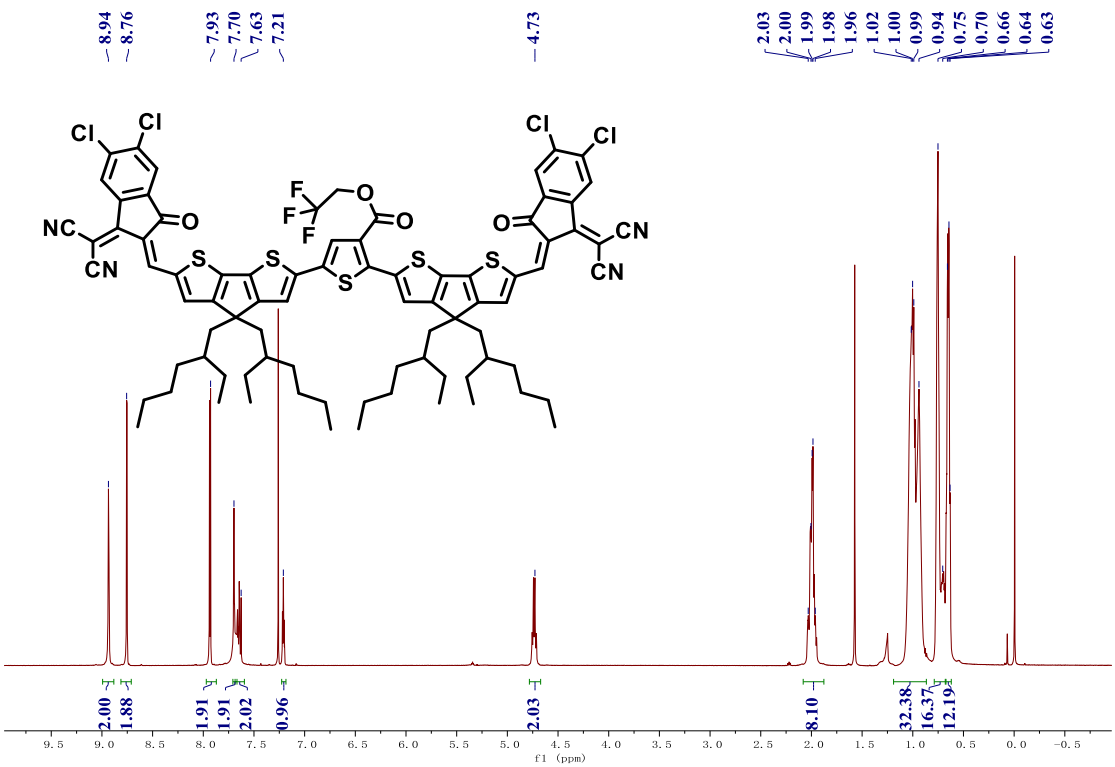


**Figure S30.** $^{1}$H NMR spectrum of compound 8c.

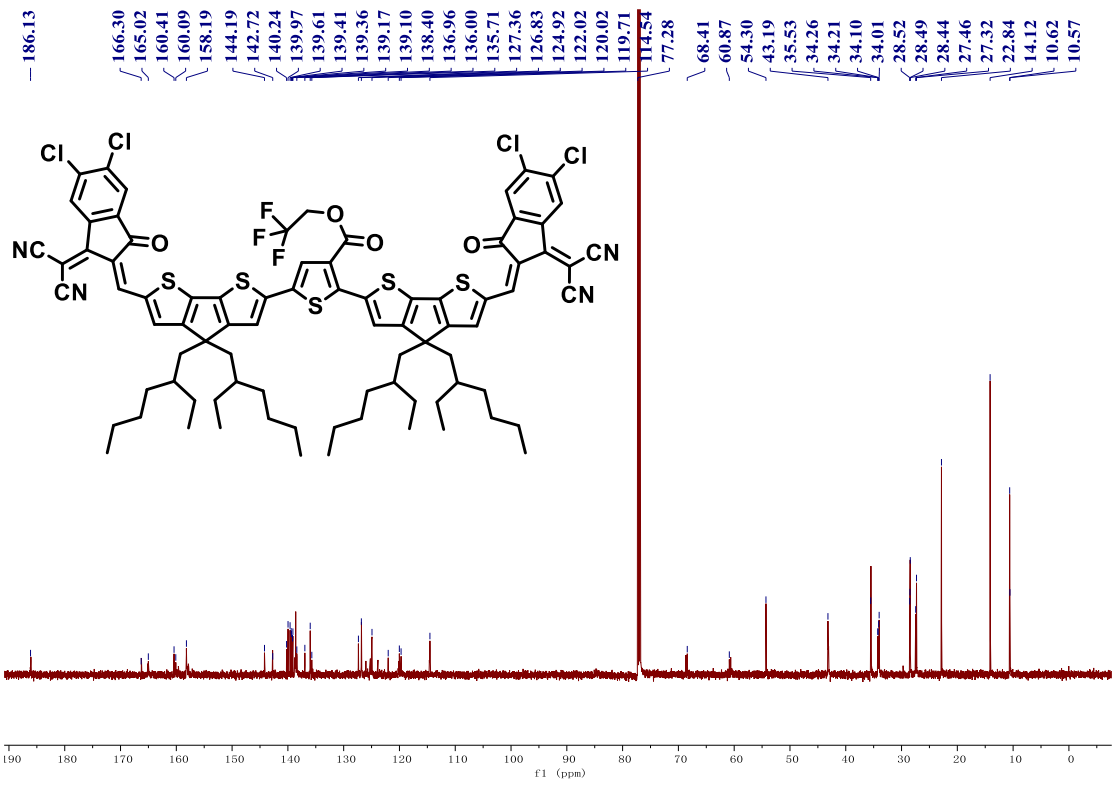


**Figure S31.** $^{13}$C NMR spectrum of compound 8c.

**Reference:**

1. Zhang, Z.; Yang, L.; Hu, Z.; Yu, J.; Liu, X.; Wang, H.; Cao, J.; Zhang, F.; Tang, W., Charge density modulation on asymmetric fused-ring acceptors for high-efficiency photovoltaic solar cells. *Materials Chemistry Frontiers* **2020,** *4* (6), 1747-1755.
2. Hexemer, A.; Bras, W.; Glossinger, J.; Schaible, E.; Gann, E.; Kirian, R.; MacDowell, A.; Church, M.; Rude, B.; Padmore, H., A SAXS/WAXS/GISAXS Beamline with Multilayer Monochromator. *J. Phys. Conf. Ser.* **2010,** *247* (1), 012007.